Theory of the propagation of high-power laser radiation in a nonlinear medium

V. N. Lugovoĭ and A. M. Prokhorov

P. N. Lebedev Physics Institute, USSR Academy of Sciences

Usp. Fiz. Nauk **111** 203–247 (October 1973)

The propagation of high-power laser beams in media with the Kerr nonlinearity is discussed allowing for various types of nonlinear absorption. A parabolic equation for the complex amplitude of the electric field is derived from the Maxwell equations under conditions of greatest practical interest. This equation is analyzed under steady-state conditions and for laser pulses of 10^{-8} sec or shorter duration. A numerical solution of the steady-state problem shows that a multifocus structure appears in a beam of supercritical power. It is shown that this multifocus structure is universal, i.e., it appears irrespective of the nature of the nonlinear absorption in the medium and of other factors allowed for in the theory. The structure of the foci is studied in detail. Within light beams such foci usually move at velocities close to that of light. A theory of moving foci is presented: The trajectories of the motion of the foci and their parameters are calculated and the broadening of the laser pulse spectra due to the motion of the foci is evaluated. Explanations are given of various experimental data on the stimulated scattering, optical breakdown, and broadening of the laser radiation spectra.

CONTENTS

I. INTRODUCTION

The propagation of high-intensity light beams in nonlinear media is attracting considerable attention. The interest in this subject is primarily due to the fact that the characteristics of the propagation of a light beam in a medium have a considerable influence on practically all the nonlinear optics phenomena investigated at present, for example, the stimulated Raman scattering, stimulated Mandel'shtam-Brillouin scattering, stimulated scattering in the wing of a Rayleigh line, optical breakdown in gases and dielectrics, broadening of the spectra of laser pulses, and so on. A correct interpretation of these phenomena is frequently based entirely on the features of the propagation of light.

Apart from these phenomena, the characteristics of the propagation of high-intensity light beams are also of basic importance. It is sufficient to compare the situation with that in linear optics whose development could have hardly taken place without the knowledge of the principal features governing the propagation of light in linear media. An equally important role in the development of nonlinear optics is played by the nature of the propagation of light in nonlinear media. Light beams generated by pulsed lasers are of greatest interest. For these beams the main contribution to the nonlinearity of a medium is made by the practically instantaneous Kerr effect.[1)] Therefore, most of the investigations of the propagation of light in the nonlinear media, following the first paper of Chiao, Garmire, and Townes[2] published in 1964, are concerned with the Kerr nonlinearity in which the refractive index of a medium becomes a function of the intensity of light.

Chiao, Garmire, and Townes[2] introduced the concept of a critical beam power. In 1965 Kelley[3] showed that the initial stages of the propagation of a light beam of supercritical power in a medium with the Kerr nonlinearity are as follows: the intensity on the beam axis rises without limit (within the framework of the parabolic equation employed) on approach to some point on the axis known as the point of collapse. However, the propagation of the beam beyond this point was not considered by Kelley. At that time the generally accepted point of view was that beyond the point of collapse a beam experiences self-trapping and travels in a waveguide manner[2] (Chiao, Garmire, and Townes[2] calculated the intensity profile of a beam traveling in a guided manner in a Kerr medium). The experimental observations of thin light filaments in liquids, glasses, and lately in gases have been regarded as a confirmation of the waveguide propagation. It should be noted that the possibility of self-trapping of an electromagnetic beam in a waveguide manner was pointed out back in 1958 by Volkov,[4] who was the first to calculate the intensity profile of a beam self-trapped in a plasma. Later the possibility of self-trapping was mentioned in[5,6] (the intensity profile considered in[6] was identical with that obtained in[4]).

However, many experimental results cannot be explained on the assumption of self-trapping of a beam into a waveguide regime beyond the point of collapse. First

of all, this assumption does not explain the very short "lifetime" of a filament which is typically of the order of 10^{-10} sec for giant laser pulses. Secondly, the length of filaments in substances such as carbon disulfide, toluene, nitrobenzene, and others has been found to exceed 5—10 cm. It is not clear how such filaments can form under the conditions of strong stimulated Raman scattering which develops in such media. In fact, according to several experimental investigations up to 90% of the energy at the end of a cuvette is pumped from a filament into the Stokes component of the scattering. According to calculations, such pumping should occur over distances of the order of 0.1 cm, which is in conflict with the observed lengths of 5—10 cm. Moreover, the nature of the emission of the anti-Stokes components of the stimulated Raman scatetring cannot be explained satisfactorily. According to the waveguide theory the vertex angles of the cones of the anti-Stokes components should be governed by Cherenkov-type conditions (see[7,8]). In fact, the emission is not of the Cherenkov type but intermediate between the Cherenkov and "volume" mechanisms of the emission of these components. Loy and Shen[9] observed ultrashort pulses in the backward stimulated Raman scattering inside a cuvette containing the investigated substance. The appearance of these pulses could not be explained by the waveguide theory of the propagation of a beam. Difficulties are also encountered when this theory is used to explain the discrete nature of the optical breakdown in transparent media, some features of the broadening of the spectra of laser pulses transmitted through matter, and other phenomena.

In 1967 Dyshko, Lugovoĭ, and Prokhorov[10] solved the problem numerically and suggested a new (multifocus) mechanism of the propagation of light beams in media exhibiting the Kerr nonlinearity.

In 1968 Lugovoĭ and Prokhorov[11] explained thin light filaments observed in earlier experiments as due to the trajectories of moving foci and not due to the waveguide propagation. This new point of view on the principal features of the propagation of light beams in nonlinear media removed all the contradictions and explained many experimental results.

The steady-state multifocus structure of a light beam represents a finite row of foci on the beam axis formed as a result of successive focusing of different ring zones in the beam. The point of collapse is not the beginning of a waveguide filament but the center of the first focus. A detailed investigation[12] of the influence of various types of nonlinear absorption in a medium,[11] i.e., of the imaginary part of the refractive index, on the propagation of a beam indicated that a multifocus structure appears irrespective of the actual nature of such absorption. A study was also made of the influence of possible deviations from the quadratic dependence of the real part of the refractive index on the field which may arise under real conditions due to the saturation of the Kerr nonlinearity (see[13-17]) or due to the nonlinear absorption in a medium. Numerical calculations were used to show that the multifocus structure of a light beam is not basically affected by such deviations and only small corrections are needed to the parameters of the foci. Thus, the multifocus propagation of light beams in media with the Kerr nonlinearity is universal, i.e., it should be observed in a great variety of physical situations.

Under real conditions an incident beam is not stationary. The beam power varies with time in accordance with the laser pulse envelope. Since the positions of the foci along the beam axis depend on the initial power and the power itself varies with time, the foci move along the beam axis. Typical velocities of the foci are of the order of 10^9 cm/sec for giant laser pulses. If the propagation pattern is recorded laterally on a photographic film, the integrated result of the motion of the foci is a thin filament, which is the trace of the foci. According to the multifocus theory the transverse dimensions of such filaments are governed by the transverse dimensions of the foci and the lifetime of these filaments represents simply the transit time of the foci across a medium to its exit plane. The calculated value of the transit time is typically 10^{-10} sec (see[11]), in full agreement with the experimental values of the filament "lifetimes."

Thus, a consistent theory of the propagation of high-power laser beams in media with the Kerr nonlinearity predicts a multifocus pattern and moving foci. This theory starts with the Maxwell equations and it is developed below.

II. INVESTIGATION METHODS AND SOME RESULTS OF STUDIES OF THE PROPAGATION OF HIGH-POWER LASER PULSES IN MATTER

1. Initial equations

The propagation of light waves in a nonlinear medium is described by the Maxwell equations

$$\operatorname{rot}\tilde{\mathbf{E}}=-\frac{1}{c}\frac{\partial\tilde{\mathbf{H}}}{\partial t},\quad \operatorname{rot}\tilde{\mathbf{H}}=\frac{1}{c}\frac{\partial\tilde{\mathbf{D}}}{\partial t},\quad \operatorname{div}\tilde{\mathbf{D}}=0 \tag{1}$$

and the constitutive equation describing the nonlinear relationship between the electric induction vector $\tilde{\mathbf{D}}$ and the electric field vector $\tilde{\mathbf{E}}$, which can be written in the form

$$\tilde{\mathbf{D}}=\varepsilon\tilde{\mathbf{E}}, \tag{2}$$

where ϵ is a nonlinear functional of $\tilde{\mathbf{E}}$. The greatest interest lies in linearly polarized high-power beams generated in lasers operating under pulse conditions (pulse durations are usually of the order of 10^{-8} sec or less). Since laser pulses are very short, the striction or thermal or associated nonlinearity mechanisms cannot appear in beams of the usual diameter ($\gtrsim 0.1$—0.03 cm) because of the relatively long times required for the redistribution of the density of matter by the striction forces or by nonuniform heating.[18-21] The main contribution to the nonlinearity of a medium is then made by the orientational[2,18-23] or electron[24-26] Kerr effect.[2)] The characteristic time for the establishment of the electron Kerr effect usually does not exceed 10^{-15} sec and, therefore, the electron nonlinearity mechanism cannot appear until we reach picosecond pulse durations, i.e., durations of the order of 10^{-12} sec. For the usual giant pulses, whose duration is of the order of 10^{-8} sec, the main contribution to the nonlinearity of the medium can only be made by the orientational Kerr effect for which the characteristic establishment time is 10^{-10}—10^{-12} sec. In those cases when the establishment time of the Kerr effect τ_K is much shorter than the characteristic times of changes in the intensity of light I of a given polarization, the refractive index of a medium at any point $\mathbf{r}$ is a function of I:

$$n=n(I)=n_0+n_2'I+\ldots\quad (n_2'>0). \tag{3}$$

This yields the following expression for the permittivity

$$\varepsilon=\varepsilon(I)=\varepsilon_0+\varepsilon_2'I+\ldots\quad (\varepsilon_0=n_0^2,\ \varepsilon_2'=2n_0n_2'). \tag{4}$$

Under the conditions specified in Eq. (9) the nature of the polarization of the incident light pulses is practically unaffected by the propagation in a medium. Therefore, for the sake of simplicity, we may assume that Eqs. (3) and (4) are independent of the nature of the initial polarization.

Eliminating the magnetic field $\tilde{\mathbf{H}}$ and the electric induction $\tilde{\mathbf{D}}$ and using Eqs. (2) and (4), we obtain the following equation for the electric field $\tilde{\mathbf{E}}$:

$$\operatorname{grad}\left(\frac{\tilde{\mathbf{E}}\operatorname{grad}\varepsilon}{\varepsilon}\right)-\Delta\tilde{\mathbf{E}}+\frac{1}{c^2}\frac{\partial^2}{\partial t^2}(\varepsilon\tilde{\mathbf{E}})=0,\quad \varepsilon=\varepsilon(\langle\tilde{\mathbf{E}}^2\rangle); \tag{5}$$

here, $\langle\tilde{\mathbf{E}}^2\rangle$ is the average value of $\tilde{\mathbf{E}}^2$ over one light-wave period ($\langle\tilde{\mathbf{E}}^2\rangle \sim \mathrm{I}$). Selecting the system of coordinates in which the z axis coincides with the central direction of propagation of a light beam, assuming that

$$\tilde{\mathbf{E}}=\tfrac{1}{2}\mathbf{E}(\mathbf{r},\,t)\,e^{ikz-i\omega t}+\text{c.c.}, \tag{6}$$

where $k = (\omega/c)\sqrt{\epsilon_0}$ and ω is the central frequency of the field oscillations in the beam, and bearing in mind that $\langle\mathbf{E}^2\rangle \ll |\mathbf{E}|^2$, we obtain the following exact equation for a new unknown function $\mathbf{E}$:

$$\frac{ik}{\varepsilon}(\mathbf{E}\operatorname{grad}\varepsilon)+\operatorname{grad}\left(\frac{\mathbf{E}\operatorname{grad}\varepsilon}{\varepsilon}\right)-\Big[\Delta\mathbf{E}+2ik\frac{\partial\mathbf{E}}{\partial z}+\left(\frac{\omega}{c}\right)^2(\delta\varepsilon)\,\mathbf{E}$$
$$+\frac{\varepsilon}{c^2}\left(2i\omega\frac{\partial\mathbf{E}}{\partial t}-\frac{\partial^2\mathbf{E}}{\partial t^2}\right)+\frac{2}{c^2}\frac{\partial\varepsilon}{\partial t}\left(i\omega\mathbf{E}-\frac{\partial\mathbf{E}}{\partial t}\right)-\frac{1}{c^2}\frac{\partial^2\varepsilon}{\partial t^2}\mathbf{E}\Big]=0, \tag{7}$$

$$\varepsilon=\varepsilon(|\mathbf{E}|^2)=\varepsilon_0+\frac{1}{2}\varepsilon_2|\mathbf{E}|^2+\ldots,\quad \delta\varepsilon=\varepsilon-\varepsilon_0=\frac{1}{2}\varepsilon_2|\mathbf{E}|^2+\ldots\quad(\varepsilon_2>0); \tag{8}$$

here, the vector $\mathbf{k}$ has the magnitude k and is directed along the z axis.

We shall assume that the following conditions, which are most interesting from the practical point of view, are satisfied for all values of $\mathbf{r}$ and t:

$$|\delta\varepsilon| \ll \varepsilon_0, \tag{9a}$$

$$\lambda \ll \Lambda_\perp \ll \Lambda_\parallel, \tag{9b}$$

$$\frac{\Lambda_\perp}{\lambda}T \ll \tau, \tag{9c}$$

$$\tau_K \ll \tau, \tag{9d}$$

where $\Lambda_\parallel$ and $\Lambda_\perp$ are the characteristic scales of the variation of the amplitude $\mathbf{E}$ along the z axis and at right-angles to this axis, respectively; τ is the scale of the variation of $\mathbf{E}$ as a function of t; $\lambda = 2\pi/k$ is the wavelength of light; $T = 2\pi/\omega$ is the period of the light wave; τ_K is the characteristic time for the establishment of the Kerr effect in a medium. The condition (9d) allows us to express the permittivity in the form given by Eq. (9). If the conditions (9a)–(9c) are obeyed, some of the terms in Eq. (7) are negligibly small. We shall first consider the projection of the vector equation (7) onto the (x, y) plane. In this case the first term vanishes. If we then assume that

$$\frac{\partial\varepsilon}{\partial\mathbf{r}_\perp}=\frac{\partial\varepsilon}{\partial|\mathbf{E}|^2}\frac{\partial|\mathbf{E}|^2}{\partial\mathbf{r}_\perp}\sim\frac{\delta\varepsilon}{\Lambda_\perp}$$

(and, similarly, $\partial\epsilon/\partial t \sim \delta\epsilon/\tau$), estimates of the remaining terms give

$$\left|\operatorname{grad}_\perp\left(\frac{\mathbf{E}\operatorname{grad}\varepsilon}{\varepsilon}\right)\right|\sim\frac{\delta\varepsilon}{\varepsilon_0}\frac{E}{\Lambda_\perp^2},\quad \Delta_\perp\mathbf{E}_\perp\sim\frac{\mathbf{E}_\perp}{\Lambda_\perp^2},\quad \frac{\partial^2\mathbf{E}_\perp}{\partial z^2}\sim\frac{\mathbf{E}_\perp}{\Lambda_\parallel^2},$$
$$2ik\frac{\partial\mathbf{E}_\perp}{\partial z}\sim i\frac{4\pi\mathbf{E}_\perp}{\lambda\Lambda_\parallel},\quad \left(\frac{\omega}{c}\right)^2(\delta\varepsilon)\,\mathbf{E}_\perp\sim\frac{4\pi^2}{\lambda^2}(\delta\varepsilon)\,\mathbf{E}_\perp,$$
$$\frac{\varepsilon}{c^2}2i\omega\frac{\partial\mathbf{E}_\perp}{\partial t}\sim 4\pi i\frac{\varepsilon_0 T}{\lambda^2\tau}\mathbf{E}_\perp,\quad \frac{\varepsilon}{c^2}\frac{\partial^2\mathbf{E}_\perp}{\partial t^2}\sim\frac{\varepsilon_0 T^2}{\lambda^2\tau^2}\mathbf{E}_\perp,$$
$$\frac{2}{c^2}\frac{\partial\varepsilon}{\partial t}i\omega\mathbf{E}_\perp\sim 4\pi i\frac{(\delta\varepsilon)\,T}{\lambda^2\tau}\mathbf{E}_\perp,\quad \frac{2}{c^2}\frac{\partial\varepsilon}{\partial t}\frac{\partial\mathbf{E}_\perp}{\partial t}\sim 2\frac{(\delta\varepsilon)\,T^2}{\lambda^2\tau^2}\mathbf{E}_\perp,$$
$$\frac{1}{c^2}\frac{\partial^2\varepsilon}{\partial t^2}\mathbf{E}_\perp\sim\frac{(\delta\varepsilon)\,T^2}{\lambda^2\tau^2}\mathbf{E}_\perp$$

[$\mathbf{E}_\perp = (\mathbf{E}_x, \mathbf{E}_y)$ and $\Delta_\perp = \partial^2/\partial x^2 + \partial^2/\partial y^2$]. Therefore, to within higher-order small terms, we obtain the following equation for $\mathbf{E}_\perp$:

$$\Delta_\perp\mathbf{E}_\perp+2ik\left(\frac{\partial\mathbf{E}_\perp}{\partial z}+\frac{1}{v}\frac{\partial\mathbf{E}_\perp}{\partial t}\right)+k^2\frac{(\delta\varepsilon)}{\varepsilon_0}\mathbf{E}_\perp=0,\quad v=\frac{c}{n_0}; \tag{10}$$

here, $\delta\epsilon = \delta\epsilon(|\mathbf{E}_\perp|^2 + |\mathbf{E}_z|^2)$. The equation obtained by the projection of the vector equation (7) onto the z axis closes the system of equations for $\mathbf{E}_x$, $\mathbf{E}_y$, and $\mathbf{E}_z$. However, it is more convenient to derive the third equation directly from $\operatorname{div}(\epsilon\mathbf{E}e^{ikz-i\omega t}) = 0$ [see Eqs. (1), (2), and (6)], which yields

$$E_z=\frac{i}{k\varepsilon}\operatorname{div}(\varepsilon\mathbf{E}). \tag{11}$$

It follows immediately from Eq. (11) that if the conditions (9a) and (9b) are satisfied for all values of $\mathbf{r}$ and t, we have

$$|E_z| \ll |\mathbf{E}_\perp|. \tag{12}$$

Then, to within terms of higher orders of smallness, we obtain

$$E_z=\frac{i}{k}\left(\frac{\partial E_x}{\partial x}+\frac{\partial E_y}{\partial y}\right). \tag{13}$$

If we use Eq. (12), we can substitute $\delta\epsilon = \delta\epsilon(|\mathbf{E}_\perp|^2)$ into Eq. (10). Thus, the propagation of a light beam in a nonlinear medium subject to the conditions (9) is described by the parabolic equation (10) for the transverse component $\mathbf{E}$ of the electric field in the beam.[3)] The longitudinal component $\mathbf{E}_z$ can be found in the first approximation using Eq. (13) and the known solution of Eq. (10).

It follows immediately from Eq. (10) for $\mathbf{E}_\perp$ that if the initial plane z = 0 the field has a definite and constant polarization for all values of t. This polarization is retained also in the space $z > 0$, i.e., it is retained during the propagation of a beam in a nonlinear medium. In particular, the propagation of linearly polarized light beams generated by pulsed lasers is described by an equation for one component of the field, for example the component $\mathbf{E}_x \equiv E$ (we recall that the x axis is selected along the electric field vector in a beam):

$$\Delta_\perp E+2ik\left(\frac{\partial E}{\partial z}+\frac{1}{v}\frac{\partial E}{\partial t}\right)+k^2\frac{\delta\varepsilon(|E|^2)}{\varepsilon_0}E=0. \tag{14}$$

The function $\delta\epsilon(|\mathbf{E}|^2)$, which occurs in the above equation, has the following simple form for media exhibiting a strong Kerr effect:

$$\delta\varepsilon(|E|^2)=\frac{1}{2}\varepsilon_2|E|^2. \tag{15}$$

The above expression represents the first term in the expansion of the quantity $\delta\epsilon$ as a series in powers of $|\mathbf{E}|^2$. The refractive index n is now given by

$$n=n_0\left(1+\frac{1}{2}n_2|E|^2\right),\quad n_2=\frac{\varepsilon_2}{2\varepsilon_0}. \tag{16}$$

The nonlinearity of the medium expressed in the form of Eq. (15) or Eq. (16) is usually called the Kerr nonlinearity. The dependence $n(|\mathbf{E}|^2)$ for large values of $|\mathbf{E}|^2$, when $|\mathbf{E}|^2 \gtrsim 1/n_2$, i.e., when Eq. (16) ceases to be valid, has been discussed in detail in[15] and elsewhere[4)] and it has been approximated in several papers[30,31] by the function

$$n=n_0\left[1+\frac{1}{2}\frac{n_2|E|^2}{1+(|E|^2/|E_s|^2)}\right] \tag{17}$$

or by other functions[32] which do not differ basically from Eq. (17). It follows from Eq. (17) that the dependence of n or ϵ on $|\mathbf{E}|^2$ disappears for $|\mathbf{E}|^2 \gg |\mathbf{E}_s|^2$. In the latter case it is usual to speak of the growth of the

Kerr nonlinearity. However, since $|E_S|^2 \sim 1/n_2$ (and this is due to the nonresonant nature of the Kerr effect), it follows from the condition (9a) that Eq. (14) is valid only for $|E|^2 \ll |E_S|^2$ when the saturation of the nonlinearity is practically absent, i.e., when the Eqs. (15) and (16) are valid. Therefore, in order to describe the propagation of light beams in the case of significant saturation of the Kerr nonlinearity of a medium we must use directly the Maxwell equations and not Eq. (14). In Sec. 1 of Chap. III we shall show that this is true also under steady-state conditions when $\partial E/\partial t \equiv 0$.[5)]

In the case of very small values of $|E|^2$ Eqs. (15) and (16) can be regarded as real. However, attention is drawn in[11] to the point that in the case of propagation of light beams in nonlinear media when the values of $|E|^2$ can be relatively high (in spite of $|E|^2 \ll |E_S|^2$), it is generally necessary to allow not only for the real part of the permittivity $\delta\epsilon'$ but also for the imaginary part $\delta\epsilon''$ associated with the nonlinear absorption in the medium. In general, the quantity $\delta\epsilon''$ is a nonlinear functional of E. However, if the main nonlinear absorption mechanism is of the many-photon type, whose characteristic establishment time usually does not exceed 10^{-15} sec, we find that both the real part $\delta\epsilon'$ and the imaginary part $\delta\epsilon''$ can be described, subject to the condition (9c), in the simple form of a function of $|E|^2$. In the case when the main nonlinear absorption mechanism is due to, for example, pumping of the energy from the beam under consideration to the stimulated scattering components, the dependence of $\delta\epsilon''$ on E does not reduce to the function of $|E|^2$ (see Sec. 2b in Chap. III). Thus, the quantity $\delta\epsilon$ occurring in Eq. (14) can be expressed in the form

$$\delta\varepsilon = \frac{1}{2}\varepsilon_2 |E|^2 + i\delta\varepsilon''. \tag{18}$$

In several cases of practical interest we find that

$$\frac{\Lambda_\parallel}{\tau} \ll v, \tag{19}$$

so that the term $(1/v)\partial E/\partial t$ in Eq. (14) is small compared with the term $\partial E/\partial z$. Ignoring the first of these terms, we obtain an equation which does not contain time explicitly:

$$\Delta_\perp E + 2ik\frac{\partial E}{\partial z} + k^2\frac{\delta\varepsilon}{\varepsilon_0}E = 0. \tag{20}$$

In this case the time dependence remains only in the boundary condition

$$E|_{z=0} = \varphi(\mathbf{r}_\perp, t), \tag{21}$$

where $\varphi(\mathbf{r}_\perp, t)$ is a given function which is governed by the electric field of a light pulse incident on the boundary z = 0. Thus, the solution of the initial transient (nonstationary) problem subject to the condition (19) reduces to the solution of the stationary problem (20)–(21), where the time t is simply a parameter in the boundary condition. Therefore, we shall start by considering the stationary (steady-state) problem. The conditions under which the inequality (19) is valid will be called quasistationary.

2. Analytic investigation

The case of an axially symmetric beam is of the greatest practical interest. The deviation $r_\perp$ from the axis of the beam will be denoted simply by r. For the sake of simplicity we shall assume that

$$\delta\varepsilon'' = \varepsilon_0 m(|E|^2) \quad (m(0) = 0) \tag{22}$$

and we shall discuss the specific case when a beam incident on the boundary of a nonlinear medium has a plane phase front and a Gaussian distribution of the intensity. Then, Eq. (20) becomes

$$\frac{\partial^2 E}{\partial r^2} + \frac{1}{r}\frac{\partial E}{\partial r} + 2ik\frac{\partial E}{\partial z} + k^2[n_2|E|^2 + im(|E|^2)]E = 0 \tag{23}$$

subject to the boundary condition

$$E|_{z=0} = E_0 e^{-r^2/2\bar{a}_0^2}; \tag{24}$$

here, the field E_0 is a parameter and the quantity $\bar{a}_0$ is the initial radius of the beam.

In the analytic investigation we shall represent the field E in the form

$$E = e^A. \tag{25}$$

Equation (23) yields the following equation for A:

$$\frac{\partial^2 A}{\partial r^2} + \frac{1}{r}\frac{\partial A}{\partial r} + \left(\frac{\partial A}{\partial r}\right)^2 + 2ik\frac{\partial A}{\partial z} + k^2[n_2 e^{2A^r} + im(e^{2A^r})] = 0 \tag{26}$$

(A^r = Re A). We shall assume that the quantity A is an analytic function of x and y. Then, the expansion of A as a Taylor series consists solely of integral nonnegative powers of the quantity $q = x^2 + y^2$:

$$A(q, z) = A_0(z) + qA_1(z) + q^2A_2(z) + \ldots \tag{27}$$

Substituting Eq. (27) into Eq. (26), we obtain the following system of equations for $A_n(z)$:

$$2ik\frac{\partial A_{n-1}}{\partial z} + 4\left[n^2A_n + \sum_{k=0}^{n} k(n-k)A_kA_{n-k}\right] + k^2n_2e^{2A_0^r}(L_{n-1} + iM_{n-1}) = 0 \quad (n = 1, 2, \ldots), \tag{28}$$

where the real coefficients $L_k(z)$ and $M_k(z)$ are given by

$$\exp[2(qA_1^r + q^2A_2^r + \ldots)] = 1 + qL_1 + q^2L_2 + \ldots,$$
$$n_2^{-1}\exp(-2A_0^r)\, m[\exp(2A_0^r + 2qA_1^r + 2q^2A_2^r)] = M_0 + qM_1 + q^2M_2 + \ldots \tag{29}$$

Introducing the notation

$$a_0 = e^{2A_0^r},\ b_0 = \frac{1}{k}\frac{dA_0^i}{dz},\ k^{-2m}A_m = a_m + ib_m,\ A^i = \mathrm{Im}\,A \quad (m = 1, 2, \ldots), \tag{30}$$

we find that Eq. (28) yields

$$2b_0 = n_2a_0 + 4a_1. \tag{31}$$

The relationship (31) gives the correction to the longitudinal wave number on the axis of the beam. For the other coefficients a_k and b_k Eq. (28) reduces to an infinite system of equations. The main properties of this system will be determined by assuming that $m(|E|^2) = 0$, i.e., we shall ignore the absorption in the medium. In this case the infinite system of equations becomes

$$\left.\begin{aligned}
&a_0' + 4b_1a_0 = 0,\\
&a_1' + 4b_1a_1 = -8b_2,\\
&b_1' + 2b_1^2 = n_2a_0a_1 + 2a_1^2 + 8a_2,\\
&a_2' + 8b_1a_2 = -8a_1b_2 - 18b_3,\\
&b_2' + 8b_1b_2 = n_2a_0(a_1^2 + a_2) + 8a_1a_2 + 18a_3,\\
&a_3' + 12b_1a_3 = -4(3a_1b_3 + 4a_2b_2) - 32b_4,\\
&b_3' + 12b_1b_3 = n_2a_0\left(\tfrac{2}{3}a_1^2 + 2a_1a_2 + a_3\right) + 8(a_2^2 - b_2^2) + 12a_1a_3 + 32a_4,\\
&a_4' + 16b_1a_4 = -8(2a_1b_4 + 3a_2b_3 + 3a_3b_2) - 50b_5 \ \text{ etc.};
\end{aligned}\right\} \tag{32}$$

here a prime represents a derivative with respect to u = kz.

We shall first consider the case when the medium is linear, i.e., $n_2 = 0$. In this case we can see that the system (32) has a class of solutions such that $a_2 \equiv b_2 \equiv a_3 \equiv b_3 \equiv \ldots \equiv 0$, and the remaining quantities (a_0, a_1, b_1) satisfy the following equations:

$$a_0' + 4b_1a_0 = 0, \quad a_1' + 4b_1a_1 = 0, \quad b_1' + 2b_1^2 = 8a_1^2. \tag{33}$$

According to Eqs. (25), (27), and (30), this class of solu-

tions corresponds to Gaussian beams and the existence of this class means that the Gaussian form of such beams is conserved during propagation in a linear homogeneous medium: such propagation changes only the width of the intensity distribution in the transverse direction (coefficient a_1), intensity on the axis (coefficient a_0), and curvature of the phase front (coefficient b_1). The general solution of the expressions in Eq. (33) yields the following relationship for the amplitude E:

$$E=\frac{E_0}{1-(z/R)+i\,(z/l_d)}\exp\left[-\frac{(1/2\bar{a}_0^2)+i\,(k/2R)}{1-(z/R)+i\,(z/l_d)}\,r^2\right], \qquad (34)$$

where

$$l_d=k\bar{a}_0^2. \qquad (35)$$

In the special case of $1/R = 0$ the solution of Eq. (34) satisfies the boundary condition (24). It is clear from Eq. (34) that the nonzero values of $1/R$ correspond to the more general boundary condition

$$E|_{z=0}=E_0\exp\left[-\frac{1}{2}\left(\frac{1}{\bar{a}_0^2}+i\,\frac{k}{R}\right)r^2\right], \qquad (36)$$

which is applicable to a focused beam such that the rays converge geometrically at a point $z = R$.

In the case of a nonlinear medium, when $n_2 \neq 0$, the situation is quite different: the class of solutions corresponding to Gaussian beams no longer exists. Even when the initial distribution is Gaussian, the propagation of a beam in a nonlinear medium results in a change in the form of this distribution i.e., it results in the appearance of nonzero coefficients a_2, b_2, a_3, b_3, ... We shall expand the coefficients a_k as a Taylor series in powers of u: $a_k = \sum_n a_k^{(n)}u^n$. Using Eqs. (28) and (32), we can show that in order to determine the coefficient $a_0^{(n)}$ for $n_2 \neq 0$ we need $2n - 1$ relationships such as the first equation in the system (32) and we need $2n + 1$ such expressions for the determination of the coefficient $a_1^{(n)}$. It is shown in[33] that this circumstance has a fundamental influence on the nature of the solution subject to the condition

$$E_0 \gg E_{cr}, \qquad (37)$$

where

$$E_{cr}=\frac{1}{\sqrt{n_2(k\bar{a}_0)^2}}. \qquad (38)$$

The condition (37) can be written also in the form

$$P \gg P_{cr}, \qquad (39)$$

where $P = (cn_0/8\pi)\int|E|^2 d\mathbf{r}_\perp$ is the beam power and

$$P_{cr}=\frac{cn_0}{2n_2k^2}. \qquad (40)$$

Thus, the condition obtained in[2] for a significant influence of the nonlinearity of a medium agrees with the condition (39) which corresponds to the case when a redistribution of the intensity of a beam in its transverse cross section begins to play an important role in the propagation process. This point has been ignored in[34] (see also review[14]) so that the correct description of the propagation of a beam in a nonlinear medium has not been provided. A similar objection applies also to a recent paper[35] in which a beam traveling in a nonlinear medium is assumed to be Gaussian.

A correct analytic solution of the problem under consideration is given in[33] but it is valid only if $|N - 1| \ll 1$, $z \ll k\bar{a}_0^2$ ($N = E_0/E_{cr}$), i.e., in a certain range of values near the initial field E_0 and only close to the boundary of the medium. For $r = 0$ this solution is of the form

$$\frac{|E|^2}{E_0^2}=1+\frac{N^2-1}{(k\bar{a}_0^2)^2}z^2-\frac{11}{3(k\bar{a}_0^2)^4}z^4. \qquad (41)$$

If $E_0^2 \gg E_{cr}^2$, we find that Eq. (32) yields

$$\frac{|E|^2}{E_0^2}=1+\frac{n_2E_0^2}{\bar{a}_0^2}z^2+\ldots, \qquad (42)$$

which governs the characteristic length l_x of the initial variation of the axial field $|E|$ along the z axis:

$$l_x=\frac{\bar{a}_0}{\sqrt{n_2E_0^2}}. \qquad (43)$$

Equation (43) was first obtained in[3].

In view of their limited validity, the analytic results do not predict several important features of the propagation of a beam in a nonlinear medium (this will be shown later). Therefore, we must consider a numerical solution of the same problem.

3. Numerical solution of the parabolic equation in the absence of absorption in a medium

We shall now consider the numerical solution of Eq. (23) subject to the boundary condition (24) and we shall assume initially, as in[3], that $m(|E|^2) \equiv 0$, i.e., we shall ignore the absorption in a nonlinear medium. For the sake of convenience we shall introduce new variables:

$$X=\frac{E}{E_0},\quad N=\frac{E_0}{E_{cr}},\quad z_1=\frac{z}{l_x},\quad r_1=\frac{r}{\bar{a}_0}, \qquad (44)$$

where E_{cr} and l_x are described by Eqs. (38) and (43). We thus obtained the following equation for the quantity X:

$$\frac{\partial^2X}{\partial r_1^2}+\frac{1}{r_1}\frac{\partial X}{\partial r_1}+2iN\frac{\partial X}{\partial z_1}+N^2|X|^2X=0 \qquad (45)$$

and the boundary condition is now

$$X|_{z=0}=e^{-r_1^2/2}. \qquad (46)$$

According to[10] if $|N - 1| \ll 1$, $z_1 \ll 1$, the numerical solution of the problem (45)–(46) confirms the analytic expression (41). We find that if $N > N_1$ (where $N_1 \approx 2$), the solution[3,10,36] has an important singularity because the intensity $|X|^2$ on the axis of a beam, i.e., for $r_1 = 0$, rises without limit as a function of z_1 on approach to a point z_1^*. The expression for z_1^* obtained in[3] on the basis of approximate numerical results is of the form

$$z_1^*\approx\frac{0.7N}{N-N_1}, \qquad (47)$$

or, if we use Eqs. (44) and (38),

$$z^*\approx 0.4\,\frac{k\bar{a}_0^2}{\sqrt{P/P_{cr}-1}};$$

here, $z^* = z_1^* l_x$, P is the power of the incident beam, and P_{cr} is close to the value defined by Eq. (40).

We note that, strictly speaking, the numerical solution does not solve the problem of the existence of a mathematical singularity at $z_1 = z_1^*$ because the approach to z_1^* in the numerical calculations gives ever increasing but always finite values of $|X|^2$, which is limited by the time spent in calculations and by the size of the computer memory. In spite of that, it follows from[3,10] that the steepness of the rise of $|X|^2$ with z for $r = 0$ at values of z close to z^* is in any case sufficiently strong to violate the condition $\Lambda_{||} \gg \lambda$ [see Eq. (9)] which is essential for the validity of the parabolic equation (45) employed here. Consequently, the question of existence of a mathematical singularity in our solution is of formal nature and we shall not consider it any further. In the next chapter we shall concentrate our attention on the

factors which under real conditions can limit the rise of $|X|^2$ in the range $z_1 \to z_1^*$.

III. STEADY-STATE MULTIFOCUS STRUCTURE OF A LIGHT BEAM IN A NONLINEAR MEDIUM

1. Formulation of the problem in the presence of absorption

A numerical solution of Eq. (45) subject to the boundary condition (46) can be used to show[10] that the singularity at $z \to z^*$ does not represent all the power of the initial beam but only some part of magnitude close to the critical power P_{cr}. The scale $\Lambda_\perp$ of the spatial variation of the field E in the transverse direction is minimal near the beam axis and, in accordance with the foregoing discussion, it is given by

$$\Lambda_\perp = \sqrt{\frac{32P_{cr}\ln 2}{cn_0|E|^2}}, \tag{48}$$

which is equal to the diameter of the paraxial distribution of the beam intensity in a given transverse section. Using Eqs. (48) and (40), we immediately find that

$$\Lambda_\perp = \frac{\lambda}{2\sqrt{n_2|E|^2}}. \tag{49}$$

Therefore, if we satisfy the condition

$$\Lambda_\perp \gg \lambda, \tag{50}$$

we automatically satisfy the first of the conditions (9) for the validity of the parabolic equation.[6] We shall see later (see Sec. 3) that the inequality (50) guarantees that the condition $\Lambda_\parallel \gg \Lambda_\perp$ is also satisfied. Therefore, on approach to the point z^* the initial equation is valid as long as the inequality (50) is satisfied.[7] If the condition (50) is not satisfied, i.e., if $\Lambda_\perp \sim \lambda$, the parabolic equation becomes invalid. If we now assume that $\Lambda_\perp \sim \lambda$ at $z \to z^*$, we find from Eqs. (40) and (48) that the intensity I on the beam axis is $\sim 3\times 10^{12}-3\times 10^{14}$ W/cm^2 for typical media such as carbon disulfide, toluene, nitrobenzene, some glasses, and so on (these media are characterized by $n_2 \sim 10^{-11}-10^{-13}$ cgs esu). At these or (in most cases) lower intensities the nonlinear absorption of light may be strong. Such absorption can be due to the many-photon mechanism, pumping of the energy to the stimulated scattering components, breakdown of matter, etc. These types of nonlinear absorption can appear at intensities of the order of $10^{10}-10^{11}$ W/cm^2, as reported in many experimental investigations (see, for example,[20,37-44]). This means that the nonlinear absorption may be the main factor which limits the energy density at $z \to z^*$. Then, the minimum value of $\Lambda_\perp$ is much greater than the wavelength λ, which is again in agreement with the experimental results. The relationship $\Lambda_\perp \gg \lambda$ is obtained also from Eq. (49) if we bear in mind that the experimentally determined values of $n_2|E|^2$ are of the order of 10^{-3} (see[45]).

Under these conditions the propagation of light beams in media can be described by the parabolic equation derived above provided the quantity $\delta\epsilon$ is introduced in its complex form of Eq. (18). The imaginary part $\delta\epsilon''$ in Eq. (18) is governed by the main nonlinear absorption mechanism. We shall consider in detail three types of such absorption: a) three-photon absorption; b) absorption due to the pumping of energy to the first Stokes component of the stimulated Raman scattering; c) two-photon absorption.

2. Numerical solution of the parabolic equation in a medium with the Kerr nonlinearity and nonlinear absorption

a) Three-photon absorption. In the three-photon absorption the imaginary part of the permittivity of a medium can be written in the form

$$\delta\varepsilon'' = \varepsilon_0 m_4 |E|^4, \tag{51}$$

where m_4 is a real coefficient. Introducing the notation of Eq. (44) and also

$$\mu_4 = \frac{m_4 E_0^2}{n_2} N^2, \tag{52}$$

we find that Eqs. (22)—(24) lead to the following equation for X:

$$\frac{\partial^2 X}{\partial r_1^2} + \frac{1}{r_1}\frac{\partial X}{\partial r_1} + 2iN\frac{\partial X}{\partial z_1} + (N^2|X|^2 + i\mu_4|X|^4)X = 0 \tag{53}$$

subject to the boundary condition (46). If $\mu_4 = 0$, Eq. (53) reduces to Eq. (45). According to Eqs. (44) and (38), the parameter N is related to the power P_0 of the incident beam by

$$N = N_1\sqrt{\frac{P_0}{P_{cr}^{(1)}}}, \tag{54}$$

where

$$P_{cr}^{(1)} = \frac{cN_1^2 n_0}{8n_2 k^2} \approx P_{cr}. \tag{55}$$

We shall now give the results of a numerical solution obtained in[12] for N = 2—10, which corresponds to the range from $P_{cr}^{(1)}$ to $27P_{cr}^{(1)}$ and $10^{-3} < \mu_4 < 0.2$. We note that if $\mu_4 > 0$, the energy density at $z_1 \to z_1^*$ rises, as expected, to finite values. The results of this numerical solution show also that the process of propagation of a light beam in a medium of this type can be regarded qualitatively as the formation of a multifocus structure. This structure represents a finite series of separate foci on the axis, resulting from successive focusing of different ring zones in the beam. The point $z_1 = z_1^*$ determines the center of the focus in such a structure.

Figure 1 shows the longitudinal section of a beam traveling in a medium of the kind considered here. It is clear from this figure that there are several foci on the axis of the beam. We can also see that only a certain fraction $P_{cr}^{(1)}$ of the power passes through the first focus. The energy reaching this focus is partly absorbed nonlinearly in the medium and partly emerges from the focus in the form of a rapidly diverging ring wave which escapes from the initial beam. Part of the beam which bypasses the first focus forms the second focus. The power reaching the second focus is close to the critical value $P_{cr}^{(1)}$. As in the case of the first focus, some of the energy is absorbed nonlinearly at the second focus and some escapes in the form of a diverging ring wave. The third, fourth, and other foci are formed in the same

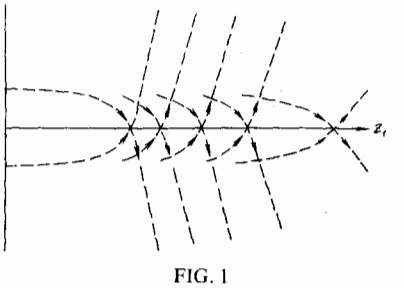

FIG. 1

manner. The passage of a beam through each focus is thus accompanied by a fall of its power by a certain amount. Consequently, the foci are formed until all the initial power is dissipated. When this happens, no further foci are formed. Thus, the total number of the foci is finite and it depends on the initial beam power. The m-th focus appears for $P = P_{cr}^{(m)}$ or, which is equivalent, for $N = N_m$. It follows from Eqs. (54) and (55) that $P_{cr}^{(m)}$ and N_m are related by

$$P_{cr}^{(m)} = \frac{cN_m^2 n_0}{8n_2 k^2}. \quad (56)$$

Numerical calculations show that if the value of the coefficient μ_4 is sufficiently small, we can estimate $P_{cr}^{(m)}$ from

$$P_{cr}^{(m)} \approx mP_{cr}^{(1)}. \quad (57)$$

More detailed information on the nature of the solution is given in Fig. 2, which shows typical dependences of $|X|^2$ and of the ratio of the beam power P at $z_1 > 0$ to the incident beam power P_0 on the value of z_1 for N = 6 and $\mu_4 = 0.05$. The three lower curves in Fig. 2 represent the dependences of $|X|^2$ on z_1 on the beam axis (i.e., for $r_1 = 0$) and on two cylinders close to the axis ($r_1 = 1/12$ and $r_1 = 1/6$) in the range $z_1 = 0.8-1.9$ (this range covers the first three foci). For the sake of convenience the curves are plotted on different scales (the scale increases with increasing r_1). The topmost curve represents the dependence of the relative power P/P_0 on z_1 in the same range of values of z_1. We can see that the dependence $|X|^2$ on z_1 for $r_1 = 0$ has three sharp peaks corresponding to three foci on the beam axis. The dependences of $|X|^2$ on z_1 for $r_1 = 1/12$ and $r_1 = 1/6$ show how the foci are formed and how the ring waves mentioned earlier emerge from the foci (the process is shown schematically by the dashed lines in the same way as in Fig. 1).

The nature of the solution at large distances from the beam axis ($r_1 \gtrsim 1$) shows that the ring waves diverging from the various foci generally interfere with the wave bypassing the foci up to z_1 and form a complex ring structure with several maxima and minima of $|X|^2$ as a function of r_1. This ring structure appears beyond the first focus, i.e., for $z_1 > z_{f1}$. The envelope of this structure can be approximated satisfactorily by a cone with a vertex angle governed by the angle of emergence of the waves from the first focus.

We shall now consider the dependence of the relative beam power P/P_0 on z_1, plotted at the top of Fig. 2. We can see that the passage of the beam through each focus is accompanied by a fall of its power P by an amount of the order of $P_{cr}^{(1)}$: in the case considered here we have N = 6 and it follows from Eq. (55) that $P_{cr}^{(1)}/P_0 \approx 0.1$. This fall of the power is obviously due to the absorption of a considerable fraction of the electromagnetic energy reaching a focal region. Therefore, it is clear that the energy flux P_{fm} through the "central" section in this region (i.e., the section $z_1 = z_{fm}$, where z_{fm} is the position of the maximum of $|X|^2$ in the m-th focal region) should represent only some fraction of $P_{cr}^{(1)}$. It follows from [12] that P_{fm} has practically the same value for all N and μ_4 and for all consecutive focal regions: this value is $P_{fm} \approx 2P_{cr}^{(1)}/3$ (the absolute precision of this value is $0.025P_{cr}^{(1)}$).

The dependence of $|X_{fm}|^2$ on μ_4, in the range of values of $|X_{fm}|^2$ considered here is close to the inverse proportionality $|X_{fm}|^2 \propto 1/\mu_4$. The nature of this relationship is illustrated in Fig. 3 which shows the dependence of $|X_{f1}|^2$ on $1/\mu_4$ for N = 6.

The total number of foci in a beam and their positions on the z_1 axis are generally functions of N and μ_4. However, in the case of sufficiently small values of μ_4 (this corresponds to a well-resolved multifocus structure in which the values of $|X_{fm}|^2$ are sufficiently large) the positions of the foci z_{fm} depend weakly on μ_4 and are close to the positions derived in [10]. In this case the positions of the foci along the z_1 axis depend strongly on the parameter N. Figure 4 shows a family of curves which represent the dependences of z_{fm} on N. In plotting these curves the parameter μ_4 was selected for each N in such a way that $|X_{f1}|^2$ was approximately 170, i.e., it was sufficiently large (the corresponding values of the ratio μ_4/N^2 are plotted as a function of N at the top of Fig. 4). For the sake of comparison, Fig. 5 shows a similar family of curves obtained in [10]. We can see

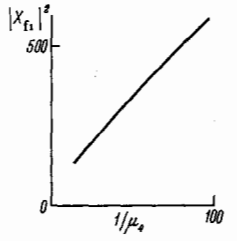

FIG. 3

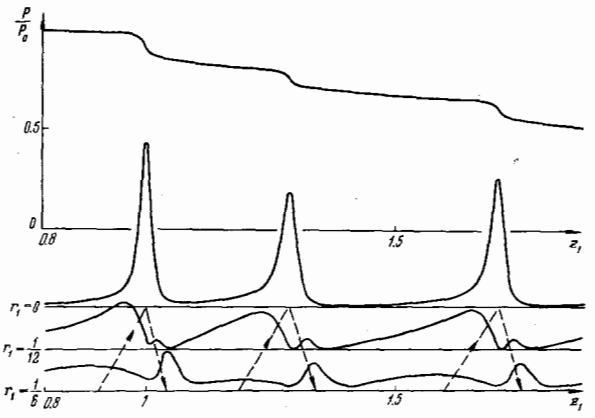

FIG. 2

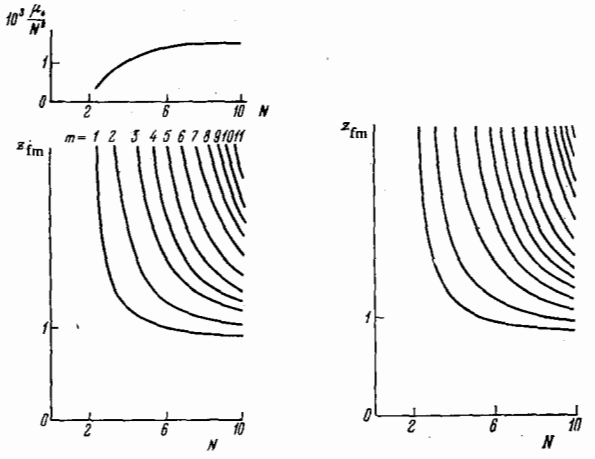

FIG. 4

FIG. 5

that these families are of the same nature and the quantitative differences between them are slight (these differences appear mainly for the foci with large values of N). The differences arise because, for the assumed values of μ_4, the power absorbed in the intervals between neighboring foci is slight but comparable with the power absorbed in the foci themselves (Fig. 2). If we reduce the value of μ_4, the power absorbed between the neighboring foci decreases and the positions of all the foci approach those given in Fig. 5. Thus, the positions of the foci z_{fm} can be approximated by the analytic dependence

$$z_{fm} = \frac{\chi_m N}{N - N_m}, \tag{58a}$$

where the quantities χ_m and N_m, which generally depend on μ_4 and N, are practically constant for sufficiently small values of μ_4. For the dimensional positions of the foci, $\zeta_{fm} = z_{fm} l_x$, Eq. (58) yields

$$\zeta_{fm} = \frac{\chi_m}{N_m} \frac{k\bar{a}_0^2}{\sqrt{P_0/P_{cr}^{(m)}} - 1}. \tag{58b}$$

Equations (58a) and (58b) with m = 1 are the more general forms of Eqs. (47) and (48). In fact, it is clear from Fig. 5 that

$$\lim_{\mu_4 \to 0} \chi_1 \approx 0.7, \text{ i.e., } \lim_{\mu_4 \to 0} z_{f1} = z_1^*. \tag{59}$$

The values of $P_{cr}^{(m)}$ and N_m, which occur in Eqs. (58a) and (58b), can easily be estimated using Eqs. (56) and (57) or, more exactly, they can be found from Eqs. (4) and (5). We shall consider the specific case corresponding to the graphs in Fig. 4. In the m = 1—4 range these graphs can be approximated satisfactorily by substituting the following values in Eqs. (58a) and (58b):

$$\begin{aligned} \chi_1 &= 0.72 \quad \chi_2 = 0.76, \\ \chi_3 &= 0.79, \quad \chi_4 = 0.77, \\ N_1 &= 1.77, \quad N_2 = 2.48, \\ N_3 &= 3.24, \quad N_4 = 3.85. \end{aligned}$$

Here, the values of N_m are close to the exact values (the differences are due to the actual method of approximation of the graphical dependences). We shall conclude this subsection by noting that the type of propagation of a light beam in a nonlinear medium discussed above is encountered also in the case of beams with other "smooth" initial intensity distributions in the transverse direction.[8)]

b) Stimulated Raman scattering in the forward direction. A consistent description of the propagation of a light beam in the presence of the stimulated Raman scattering is generally quite difficult because of the need to allow for the distribution of δ-correlated sources (nuclei) of the scattered Stokes radiation (see[48]). Therefore, we shall consider only a model situation in which the energy is pumped from the main beam solely to the first Stokes component of the stimulated Raman scattering and this component is initiated by a monochromatic "nuclear" beam incident, like the main beam, from outside on the boundary z = 0. If the Kerr effect can occur in the beam representing the first Stokes component, it follows from the coherence of this beam that independent focal regions can form in such a beam. However, we shall not consider the possibility of such situations under real conditions.[9)] Therefore, we shall consider the Kerr effect in the main beam but ignore it in the beam representing the first Stokes component. We shall assume that both beams are axially symmetric. In most cases of practical interest we also can ignore the change in the population of the vibrational ground state of the molecules in the medium under consideration.[10)] In this case the imaginary component of the permittivity of the medium in the main beam is positive and equal to $4\pi\Gamma|E_{-1}|^2$ whereas in the first Stokes component the permittivity is negative and equal to $-4\pi\Gamma|E|^2$, where E is the complex amplitude in the main beam [see Eq. (6)], E_{-1} is the complex amplitude in the first Stokes component, and Γ is a coefficient discussed in[48]. Thus, Eq. (20) for E and the corresponding equation for E_{-1} (obtained in the same approximation) are

$$\begin{aligned} \frac{\partial^2 E}{\partial r^2} + \frac{1}{r}\frac{\partial E}{\partial r} + 2ik\frac{\partial E}{\partial z} + k^2\left(n_2|E|^2 + i\frac{4\pi\Gamma}{\varepsilon_0}|E_{-1}|^2\right)E = 0, \\ \frac{\partial^2 E_{-1}}{\partial r^2} + \frac{1}{r}\frac{\partial E_{-1}}{\partial r} + 2ik_{-1}\frac{\partial E_{-1}}{\partial z} - k_{-1}^2\frac{4\pi\Gamma}{\varepsilon_0}|E|^2 E_{-1} = 0; \end{aligned} \tag{60}$$

here, $k_{-1} = 2\pi/\lambda_{-1}$; $\lambda_{-1} = 2\pi c/\omega_{-1} n_0$; $\omega_{-1} = \omega - \omega_0$ is the first Stokes frequency; ω_0 is the frequency of a vibrational transition in matter which is associated with the stimulated Raman effect.

Following Eq. (24), we shall confine ourselves to the specific case of Eq. (60) subject to the conditions

$$E|_{z=0} = E_0 e^{-r^2/2\bar{a}_0^2}, \quad E_{-1}|_{z=0} = E_{-1,0} e^{-r^2/2\bar{a}_0^2}, \tag{61}$$

which correspond to an initial Gaussian distribution of the intensities in both beams with the same radii of this distribution and with plane phase fronts of the beams in the initial transverse section. Introducing the notation of Eq. (44) and supplementing this notation with

$$H = k\bar{a}_0\sqrt{\frac{4\pi\Gamma}{\varepsilon_0}E_0^*}, \quad Y = E_{-1}/E_0, \quad \xi = \frac{k_{-1}}{k} = \frac{\omega_{-1}}{\omega},$$

we obtain the following system of equations for the dimensionless quantities X and Y:

$$\begin{aligned} \frac{\partial^2 X}{\partial r_1^2} + \frac{1}{r_1}\frac{\partial X}{\partial r_1} + 2iN\frac{\partial X}{\partial z_1} + (N^2|X|^2 + iH^2|Y|^2)X = 0, \\ \frac{\partial^2 Y}{\partial r_1^2} + \frac{1}{r_1}\frac{\partial Y}{\partial r_1} + 2iN\xi\frac{\partial Y}{\partial z_1} - i\xi^2 H^2|X|^2 Y = 0 \end{aligned} \tag{62}$$

which is subject to the boundary conditions

$$X|_{z_1=0} = e^{-r_1^2/2}, \quad Y|_{z_1=0} = \alpha e^{-r_1^2/2}, \tag{63}$$

where $\alpha = E_{-1,0}/E_0$ is the ratio of the initial field intensity on the axis of the auxiliary ("nuclear") beam to the initial intensity of the field on the axis of the main beam. The numerical solution of the problem given in[12] for $\alpha = 10^{-4}$, $\xi = 0.9$, and values of N and H in the range 4—10, has shown that for each value of N there is a critical value $H = H_{cr}(N)$ such that for $H < H_{cr}$ the value of $|X|^2$ considered as a function of z_1 on the beam axis rises without limit on approach to the first focus.[11)] If $H > H_{cr}$ this solution is fully determined for all values $z > 0$ within the range of validity of Eq. (60). If the value of H is only slightly greater than H_{cr}, the solution is a multifocus structure and the positions of the first few foci differ only slightly from the positions shown in Fig. 5. The other foci may not exist at all because a strong pumping of the energy from the main to the Stokes beam occurs in the course of propagation. This reduces the intensity of the main beam so that the tendency for the rise of the intensity on the axis in further foci is completely suppressed by the absorption.

Figure 6 shows typical dependences of $|X|^2$ on z_1 for N = 6, $H = 1.04H_{cr}$ ($H_{cr} \approx 7$). The three continuous curves in Fig. 6 give the dependences of $|X|^2$ on z_1 on the beam axis ($r_1 = 0$) and on two cylindrical surfaces $r_1 = 1/12$ and $r_1 = 1/6$ in the range $z_1 = 0.8$—1.9. Each of the curves is plotted on the same scale as the corresponding curve in Fig. 2. The dashed lines in Fig. 6

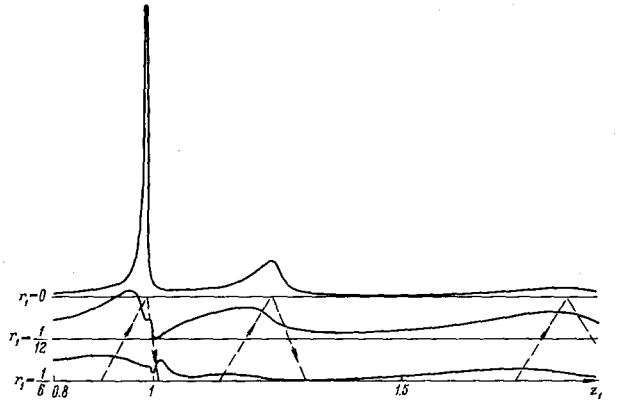

FIG. 6

represent schematically the process of formation of the foci and the emergence of ring waves (in this example the total number of foci in the main beam is three and all three foci lie in the range $z_1 = 0.8-1.9$). The power P_{fm} flowing through the central section of the m-th focal region is practically the same, $P_{fm} \approx 0.7P_{cr}^{(1)}$ (with an absolute precision of $0.01P_{cr}^{(1)}$), for all the three foci in this example. Bearing this point in mind and using the values of $|X_{fm}|^2$ shown graphically in Fig. 6, we can determine easily the dimensions of the three focal regions. We can see that these dimensions increase rapidly with the number of the focus because of the strong fall of $|X_{fm}|^2$ with increasing m. For this reason experimental observations may result in recording of only the first focus because a detector may be insufficiently sensitive for the low energy density in the second and third foci.

c) Two-photon absorption. If the main form of absorption in a medium is the two-photon process, the imaginary part of the permittivity of this medium is proportional to $|E|^2$:

$$\delta\varepsilon'' = \varepsilon_0 m_2 |E|^2. \tag{64}$$

Here, m_2 is a real coefficient. Introducing

$$\mu_2 = \frac{m_2}{n_2} N^2 \tag{65}$$

and using Eqs. (22)–(24), (44), we obtain the following equation for X:

$$\frac{\partial^2 X}{\partial r_1^2} + \frac{1}{r_1}\frac{\partial X}{\partial r_1} + 2iN\frac{\partial X}{\partial z_1} + (N^2|X|^2 + i\mu_2|X|^2)X = 0 \tag{66}$$

subject to the boundary condition (46).

A number of numerical calculations concerned with this problem[12] has shown that, in the (N, μ_2) plane, there is a curve $\mu_2 = \mu_{2cr}(N)$ such that, if $\mu_2 < \mu_{2cr}$ the value of $|X|^2$ considered as a function of z_1 on the beam axis rises without limit on approach to the first focus (as in the case $H < H_{cr}$ considered in the preceding subsection); if $\mu_2 > \mu_{2cr}$, the solution is fully determined for all values $z_1 > 0$. In the latter case, if the value of μ_2 does not exceed greatly μ_{2cr} (for example, if $\mu_{2cr} < \mu_2 < 2\mu_{cr}$), this solution represents a multifocus structure. A characteristic feature of this structure is that the positions of the foci differ considerably from the positions shown in Fig. 5. This difference is due to the fact that the two-photon absorption outside the foci is negligibly weak only for sufficiently small values of the coefficient μ_2, whereas for $\mu_2 > \mu_{2cr}$ such absorption should always be finite, i.e., the power absorbed between the neighboring foci should be finite (it should also be finite between the initial planes $z_1 = 0$ and the first focus). Consequently, the total number of the foci is considerably less than in the absence of two-photon absorption in the medium. Nevertheless, the mechanism of the formation of the foci and the beam structure are the same as in the two preceding cases.

Figure 7 shows three dependences of $|X|^2$ on z_1 for $r_1 = 0$, $r_1 = 1/12$, $r_1 = 1/6$, $N = 6$, $\mu_2 = 2.6$. Each of these curves is plotted on the same scale as the corresponding curves in Fig. 2. The range $1 < z < 2.1$ used in Fig. 7 includes the first two foci. Comparing Figs. 2 and 7, we can see that the qualitative features of the formation of the foci and the emergence of ring waves from these foci are the same for the two- and three-photon absorption cases. The dependence of the relative beam power P/P_0 on z_1, plotted at the top of Fig. 7, also shows that at each focus the absorbed power is of the order of $P_{cr}^{(1)}$. Moreover, a considerable fraction of the beam power is absorbed in the interval between the initial plane $z_1 = 0$ and the first focal region as well as between the neighboring foci. The power P_{fm} passing through the central section of the m-th focal region is $P_{f1} \approx 0.61P_{cr}^{(1)}$ and $P_{f2} \approx 0.66P_{cr}^{(1)}$ for $m = 1, 2$.

The positions of the foci z_{fm} along the z_1 axis depend on the parameters N and μ_2. Figure 8 shows a family of curves which give the dependences of z_{fm} on N for certain values of μ_2. The values of μ_2 are selected for each N in such a way that the quantity $|X_{f1}|^2$ remains constant and amounts to about 110. The dependence of the ratio μ_2/N^2 on N is also included in Fig. 8. Comparing Figs. 4 and 8 (or Figs. 2, 6, and 7) we see that in the two-photon absorption case the distances between the foci

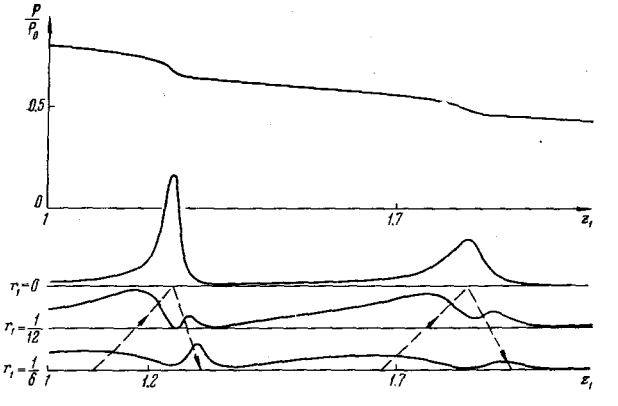

FIG. 7

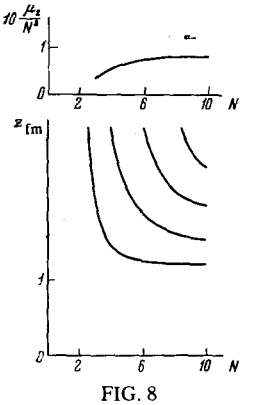

FIG. 8

may be considerably greater than for the other forms of nonlinear absorption.

Thus, the results given in the preceding subsections (a, b, c) show that the propagation of a high-power light beam in a wide range of media exhibiting the Kerr nonlinearity gives rise to a multifocus structure of the beam. It follows from[11] that the actual nature of the nonlinear absorption in a medium governs only some quantitative characteristics (values of the energy density in the focal regions, dimensions of these regions, the number of foci, and their relative positions), whereas the basic nature of the propagation of a beam is independent of the type of absorption.

A multifocus structure definitely appears in a beam if the nonlinear absorption in a medium occurs only in the focal regions, but has no significant influence on the other parts of the beam and—particularly—does not prevent the formation of the focal regions themselves. These conditions are satisfied by the three-photon absorption (subsection a) for sufficiently small values of the coefficient m_4 [see Eq. (51)]. The same conditions are also satisfied by the four-photon, five-photon, and stronger absorption provided the coefficients m_6, m_8, and so on are sufficiently small. The other types of nonlinear absorption (considered in subsections b and c) also allow the appearance of a multifocus structure of a beam even when the absorption is strong outside the focal regions. In the last case the total number of the foci and their positions on the beam axis depend strongly on the power absorbed outside the foci.

3. Structure of foci

The longitudinal structure of focal regions is characterized by the dependence of $|X|^2$ on z_1 on the beam axis ($r_1 = 0$) in the vicinity of the maxima of this quantity. This dependence is shown in Figs. 2, 6, and 7 for all three types of nonlinear absorption discussed above. It is clear from these figures that the foci with different numbers are similar and are characterized by a dependence of $|X|^2$ on z_1 which is asymmetric with respect to the maxima of this quantity (the rear slopes of the curves are steeper than the front slopes). The values of $|X|^2$ on the beam axis ($r_1 = 0$) near the m-th focal region can be approximated by

$$|X|^2 = \begin{cases} \dfrac{|X_{fm}|^2}{\{1+[(z_1-z_{fm})/\mu_m]^2\}^{\alpha}}, & z_1 \leqslant z_{fm}, \\ \dfrac{|X_{fm}|^2}{\{1+[(z_1-z_{fm})/\mu_m]^2\}^{\beta}}, & z_1 \geqslant z_{fm}, \end{cases} \tag{67}$$

where $\alpha \approx 1/2$ and the value of β is generally independent of the nature and magnitude of the nonlinear absorption (it usually lies in the range $\beta = 1-2$).

The transverse structure of the focal regions (governed by the dependence of $|X|^2$ on r_1 in the transverse sections $z_1 = z_{fm}$) is illustrated in Fig. 9 for the first three foci in the three-photon absorption case ($N = 6$, $\mu_4 = 0.05$). We can see that the transverse structures of different focal regions are similar. This similarity is understandable if we bear in mind that the mechanism of formation of all the foci is the same. This similarity of the transverse structure of the focal regions is observed also for the other types of nonlinear absorption discussed above. We shall use r_{fm} to denote the radius of the distribution of the intensity along r_1 in the m-th focal region, i.e., we shall use it to denote the value of r_1 at which $|X|^2 = (1/2)|X_{fm}|^2$. It is clear from Fig. 9

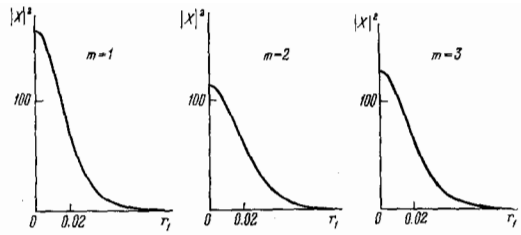

FIG. 9

that if $r_1 < r_{fm}$, the radial distribution of the intensity in the focal region is very nearly Gaussian

$$|X|^2 = |X_{fm}|^2 \exp\left[-\left(\frac{r_1}{r_{fm}}\right)^2 \ln 2\right]. \tag{68}$$

We can conveniently express Eqs. (67) and (68) in the dimensional form:

$$|E|^2_{r=0} = \begin{cases} \dfrac{|E_{fm}|^2}{\{1+[(z-\zeta_{fm})/\Lambda_{fm}]^2\}^{\alpha}}, & z \leqslant \zeta_{fm}, \\ \dfrac{|E_{fm}|^2}{\{1+[(z-\zeta_{fm})/\Lambda_{fm}]^2\}^{\beta}}, & z \geqslant \zeta_{fm}, \end{cases} \tag{69}$$

$$|E|^2_{z=\zeta_{fm}} = |E_{fm}|^2 \exp\left(-\frac{4r^2}{d_{fm}^2} \ln 2\right), \quad r \leqslant \frac{d_{fm}}{2};$$

here, $E_{fm} = E_0 X_{fm}$; $d_{fm} = 2r_{fm}\bar{a}_0$ is the diameter of the focal region; $\Lambda_{fm} = \mu_m l_x$ is the scale of the longitudinal variation of the field E in the focal region ($\Lambda_{fm} \equiv \Lambda_{||}$) related (for $\beta \sim 1-2$) to the total length l_{fm} of the focal region by

$$l_{fm} \approx 2.5\ \Lambda_{fm}. \tag{70}$$

The power flowing through the central section of any focal region is $P \approx 2P_{cr}^{(1)}/3$ irrespective of the conditions and of the nature of nonlinear absorption (Sec. 2 in Chap. III). It follows from Eq. (69) that

$$P_{fm} = \frac{cn_0 d_{fm}^2 |E_{fm}|^2}{32 \ln 2} = \frac{N^2 |X_{fm}|^2 r_{fm}^2}{N_1^2 \ln 2} P_{cr}^{(1)}. \tag{71}$$

Therefore, the values of the maximum intensity $|E_{fm}|^2$ and of the diameter d_{fm} are related by

$$|E_{fm}|^2 d_{fm}^3 \approx 0.18 \frac{\lambda^2}{n_2}. \tag{72}$$

We have allowed here for the fact that $N_1^2 \ln 2 \approx 2.7$. The values of d_{fm} are governed by the nonlinear absorption in the medium. The results plotted in Fig. 3 and 4 (see Sec. 2a in Chap. III) allow us to find the relationship between d_{f1} and the three-photon absorption coefficient m_4 for the most interesting conditions. We can easily see that if $\mu_4/N^2 \sim 2 \times 10^{-3} - 2 \times 10^{-4}$ (i.e., if $|E_{f1}|^2 \sim 100E_0^2 - 1000E_0^2$), and $N \gtrsim 4$ (i.e., $P_0 \gtrsim 4P_{cr}^{(1)}$), the energy density $|E_{f1}|^2$ at the center of the first focus is practically independent of the initial beam power and the corresponding value of $|E_{f1}|^2$ is

$$|E_{f1}|^2 \approx 0.15 \frac{n_2}{m_4}. \tag{73a}$$

i.e., it is governed only by the constants of the medium n_2 and m_4. Consequently, the diameter d_{f1} of the first focal region is also governed solely by these constants:[12)]

$$d_{f1} \approx 1.1\lambda \frac{\sqrt{m_4}}{n_2}. \tag{73b}$$

Similar relationships apply to the other foci. It should be noted that, according to the reported experimental results, the measured diameters of the foci in any given substance vary only slightly with the observational conditions and amount to 5×10^{-4} cm for carbon disulfide,

1.2×10^{-3} cm for nitrobenzene, and 10^{-3} cm for toluene.[15,51] It should also be noted that these values are obtained for ruby laser radiation ($\lambda = 0.5 \times 10^{-4}$ cm) and that they exceed greatly the value of λ.

We shall now estimate the fraction of the power absorbed in the focal regions in the case of, for example, the three-photon absorption in a medium. It follows from Eq. (51) that the ratio of the power absorbed in a focus to the power entering a focus is of the order of $km_4|E_{fm}|^2 l_{fm}$ or, if we take into account Eqs. (72) and (73a), it is of the order of l_{fm}/kd_{fm}^2. If we postulate that, in accordance with the results presented in Sec. 2, this ratio should be of the order of unity, we find that $l_{fm} \sim kd_{fm}^2$. Thus, the length of a focal region is related to its diameter in the same way as in a linear medium.[13] More accurate values of the numerical coefficient in this relationship can be obtained directly from Figs. 2, 6, and 7 and from the values of the power flowing through the central sections of the focal regions. It follows from these figures and the relevant parameters that the expressions for the three types of nonlinear absorption are

$$l_{fm} \approx 3kd_{fm}^2, \tag{74a}$$

$$l_{fm} \approx 2kd_{fm}^2, \tag{74b}$$

$$l_{fm} \approx 4kd_{fm}^2. \tag{74c}$$

It follows from these expressions that the condition $\Lambda_{\parallel} \gg \Lambda_{\perp}$ (or $l_{fm} \gg d_{fm}$) necessary for the validity of the parabolic equation [see Eq. (9)] is satisfied because $\Lambda_{\perp} \gg \lambda$ (or $d_{fm} \gg \lambda$).

We shall now consider a numerical example corresponding to typical experimental conditions. The initial radius of a beam $\bar{a}_0$ is 0.15 mm.[42,52] Wavelength λ in matter is 0.5×10^{-4} cm, which corresponds to the ruby laser radiation in a substance whose refractive index is $n_0 \approx 1.5$. We shall consider the specific case of carbon disulfide for which $n_2 \sim 0.5 \times 10^{-11}$ cgs esu. Therefore, it follows from Eqs. (55) and (40) that for this substance $P_{cr}^{(1)} \sim 20$ kW.[14] If the incident beam power is $P_0 \sim 200$ kW $\sim 10P_{cr}^{(1)}$, we find from Eq. (54) that N = 6. It follows from Eqs. (48) and (59) or directly from Figs. 4, 5, and 8 that the distances ζ_{fm} of the first few foci measured from the entry plane are 5–10 cm. It then follows from Eq. (71) that

$$|X_{fm}|^2 \approx \frac{2N_0^2 \ln 2}{3N^2 r_{fm}^2} \approx \frac{7{,}2}{N^2}\left(\frac{\bar{a}_0}{d_{fm}}\right)^2.$$

Since in the case of carbon disulfide we have $d_{f1} \approx 5 \times 10^{-4}$ cm, it follows that $|X_{f1}|^2 \approx 180$ or, which is equivalent, $|E_{f1}|^2 \approx 180E_0^2$. Thus, the example considered here lies within the range of the parameters used in the numerical calculations and those used in the corresponding analytic approximations. An estimate of the length of the focal region made using Eq. (74) gives $l_{f1} \sim 1$ mm.

Let us now consider somewhat different example. We shall assume the initial beam radius $\bar{a}_0$ is 0.5 mm. We shall consider a cuvette $l = 10$ cm long filled with a nonlinear substance. Then, it follows from Eq. (58) that the first focus appears inside the cuvette only if the initial beam power exceeds the critical value by a factor of at least 150. Clearly, for this excess of the initial power over the critical value the deviations from axial symmetry in the initial distribution in a real beam may themselves be supercritical and thus, independent multifocus structures may appear in some parts of the beam. In this case the initial radius and power for each of the structures will be considerably smaller than 0.5 mm and $150P_{cr}^{(1)}$. This splitting of the initial beam into several independent beams has been observed experimentally for a very high supercritical powers. In this case the initial radius $\bar{a}_0$ of the independent beams is of the order of 0.1 mm (see[41]) which gives $10P_{cr}^{(1)}$ for the initial power. It should be noted that the theoretical possibility of such splitting of a strongly supercritical beam was pointed out in[46,55,56].[15]

We shall now estimate the longitudinal component E_z of the electric field in the focal regions. It follows from Eqs. (13) and (69) that

$$|E_z'| = \frac{1}{k}\left|\frac{\partial E}{\partial r}\cos\varphi\right| \approx |E_{fm}\cos\varphi|\frac{4r\ln 2}{kd_{fm}^2}\exp\left(-\frac{4r^2}{d_{fm}^2}\ln 2\right), \tag{75}$$

where φ is the polar angle in a cylindrical system of coordinates r, φ. According to Eq. (75) the maximum value of $|E_z|$ corresponds to $\varphi = 0$ or $\varphi = \pi$ and $r = r_{max}$, where

$$r_{max} \approx \frac{d_{fm}}{2\ln 2}. \tag{76}$$

The corresponding maximum value $|E_z|_{max}$ is

$$|E_z|_{max} \approx 0.1\frac{\lambda}{d_{fm}}|E_{fm}|. \tag{77}$$

The amplitude of the transverse component of the electric field $|E_{fm}|$ can easily be estimated from Eq. (72). If $n_2 = 0.5 \times 10^{-11}$ cgs esu, $d_{fm} = 5 \times 10^{-4}$ cm, $\lambda = 0.5 \times 10^{-4}$ cm, we find that $|E_{fm}| \approx 1.9 \times 10^4$ cgs esu and it then follows from Eq. (77) that $|E_z|_{max} \approx 1.9 \times 10^2$ cgs esu.

We shall conclude this chapter by pointing out the propagation of light beams in media with the Kerr nonlinearity is sometimes described using geometrical optics (see[58,59]). However, this approximation is clearly inapplicable to a multifocus structure. In fact, the power reaching the first focus is $P_{f1} \approx P_{cr}^{(1)}$ and hence we obtain $l_{nl} \sim l_d$, where $l_{nl} = d_{f1}/2\sqrt{n_2}|E_{f1}|^2$ is the characteristic length of the variation of the field in the focal region due to the nonlinearity of the substance (obtained in the geometrical optics approximation); $l_d \parallel kd_{f1}^2$ is the characteristic length of the diffraction divergence in the corresponding linear medium. Since the values of l_{nl} and l_d are of the same order of magnitude, the behavior of a beam in a focal region is governed equally well by the geometrical-optics refraction due to the nonlinearity of the medium and by diffraction. Therefore, the geometrical-optics approximation loses its validity in the region of the first focus and everywhere beyond it.

IV. PROPAGATION OF HIGH-POWER LIGHT PULSES IN A NONLINEAR MEDIUM. THEORY OF MOVING FOCI

1. Quasistationary beams

According to Eqs. (20) and (21), we can analyze the propagation of a light beam in a nonlinear medium under quasistationary conditions by regarding the time t as a parameter in the boundary condition. We shall consider the specific boundary condition

$$E|_{z=0} = E_0(t)e^{-r^2/2\bar{a}_0^2} \tag{78}$$

i.e., we shall assume that for all values of t the incident beam has a Gaussian distribution of the intensity with a

constant radius $\bar{a}_0$ and a plane phase front. The function $E_0(T)$ in Eq. (78) is governed by the envelope of the laser pulse, i.e., by the time dependence of the initial beam power P_0.

We shall now analyze the solutions obtained in the preceding chapter allowing for the time dependence of the initial beam power. Since the longitudinal positions of all the foci depend strongly on this power, we can immediately see that the foci must move along the beam axis with the envelope of the laser pulse.[11] It follows from Eq. (58b) that the time dependence of the position of a focus ζ_{fm} is

$$\zeta_{fm}(t)=\frac{\chi_m}{N_m}\frac{k\bar{a}_0^2}{\sqrt{P_0(t)/P_{cr}^{(m)}-1}}; \tag{79}$$

here χ_m/N_m is a numerical coefficient [see Eq. (59)]; $P_0(t) = (cn_0/8)\bar{a}_0^2E_0^2(t)$. The total number m of the foci in the region $z > 0$ at a moment t is given by the condition $P_0(t) > P_{cr}^{(m)}$. If the maximum laser pulse power exceeds only slightly the critical value $P_{cr}^{(1)}$, only one moving focus is formed. Then, other foci appear and their number increases with the maximum initial power.

Under real conditions we are always dealing with a layer of finite thickness l which is governed, for example, by the length of a cuvette containing the substance under investigation. The moments t_m at which each focal region traverses the exit plane of the medium or any other fixed plane in the medium are different and the corresponding characteristic transit times Δt_m are given by the formula

$$\Delta t_m=\frac{l_{fm}}{|V_{fm}|}, \tag{80}$$

where V_{fm} are the velocities of the foci:

$$V_{fm}=\frac{d\zeta_{fm}}{dt}\Big|_{t=t_m}. \tag{81}$$

We shall consider the specific case of a pulse whose envelope is of the following type:

$$P_0(t)=\frac{P_{max}}{[1+(1.3t/\tau_p)^2]^2}; \tag{82}$$

Here, τ_p is the pulse duration measured at the $P_{max}/2$ level. The time is measured from the moment when the maximum of the incident power passes through z = 0 (pulses with different envelopes can be considered in exactly the same way and the results are basically the same). Then, it follows from Eq. (79) that the positions of the foci $\zeta_{fm}(t)$ are given by

$$\zeta_{fm}(t)=\chi_m k\bar{a}_0^2\frac{1+(1.3t/\tau_p)^2}{N_{max}-N_m-N_m(1.3t/\tau_p)^2}, \tag{83}$$

where $N_{max} = N_1\sqrt{P_{max}/P_{cr}^{(1)}}$. The moment t_m at which the m-th focus passes through the plane $z = l$ is obviously given by the condition $\zeta_{fm} = l$, which gives

$$t_m=\pm\frac{\tau_p}{1.3}\sqrt{\frac{N_{max}-N_m-\chi_m(k\bar{a}_0^2/l)}{N_m+\chi_m(k\bar{a}_0^2/l)}}. \tag{84}$$

We can see that the condition for the appearance of this focus in the layer under consideration ($0 \le z \le l$) reduces to the inequality $N_{max} - N_m - \chi_m(k\bar{a}_0^2/l) \ge 0$. Then, it follows from Eqs. (83) and (84) that the m-th focus appears initially in the $z = l$ section at a moment $t_m < 0$ [this corresponds to the minus sign in Eq. (84)] and moves back into the investigated layer. At t = 0 this focus is located at $z = \zeta_{min}^{(m)}$, where

$$\zeta_{min}^{(m)}=\frac{\chi_m k\bar{a}_0^2}{N_{max}-N_m}. \tag{85}$$

and then it again moves toward the boundary $z = l$. The moment t_m at which this focus leaves the layer corresponds to the plus sign in Eq. (84).

We shall now calculate the velocities of foci in a section z. It follows from Eq. (83) that

$$V_{fm}=\frac{2.6}{\tau_p}\frac{\chi_m k\bar{a}_0^2N_{max}(1.3t/\tau_p)}{[N_{max}-N_m-N_m(1.3t/\tau_p)^2]^2} \tag{86}$$
$$=\pm\frac{2.6}{\tau_p}\frac{z^2}{\chi_m k\bar{a}_0^2N_{max}}\left(N_{max}-N_m-\chi_m\frac{k\bar{a}_0^2}{z}\right)^{1/2}\left(N_m+\chi_m\frac{k\bar{a}_0^2}{z}\right)^{3/2}.$$

We can see that the absolute values of the velocities $|V_{fm}|$ increase monotonically with increasing |t| or z. The maximum velocities in the layer under investigation are reached at the boundary $z = l$. We shall estimate the velocities of the foci $|V_{fm}|$ under typical conditions and we shall find the time intervals Δt_m during which they remain at a given point in a medium. We shall assume that the parameters of a light beam and its maximum power are the same as in the first numerical example in Sec. 3 of Chap. III, i.e., we shall assume that $N_{max} = 6$ (i.e., $P_{max} \approx 10P_{cr}^{(1)}$), $\bar{a}_0 = 0.15$ mm, $\lambda = 0.5 \times 10^{-4}$ cm, $l_{fm} = 0.1$ cm (i.e., $d_{f1} \approx 5 \times 10^{-4}$ cm), $l = 10$ cm. We shall assume that the duration of the laser pulse is $\tau_p = 2 \times 10^{-8}$ sec. Then, at a distance $z = l = 10$ cm from the entry plane it follows from Eqs. (86) and (59) that

$$|v_{f1}| \approx |v_{f2}| \approx 1.2\cdot10^9 \text{ cm/sec}, \qquad |v_{f3}| \approx 0.9\cdot10^9 \text{ cm/sec}.$$

Hence, we find from Eq. (80) that $\Delta_{tm} \approx 10^{-10}$ sec. It is clear from these estimates that the characteristic times Δt_m which determine the scale of τ [see Eq. (9)] are considerably longer than the establishment time of the orientational Kerr effect. For example, in the case of carbon disulfide the establishment time of the orientational Kerr effect is $\tau_K < 2 \times 10^{-12}$ sec.[45] Therefore, the condition (9d) of the validity of the initial equation is known to be satisfied even for the orientational mechanism of the Kerr effect. In such situations this condition is satisfied also for the orientational Kerr effect in other substances. The same condition is satisfied by a large margin in the case of the electron Kerr effect. We can easily see that the condition (9c) is also satisfied. We shall now consider the last of the conditions of the validity of Eq. (20), represented by the inequality (19). This inequality can be rewritten in the form

$$|V_{fm}| \ll v, \tag{87}$$

where v is the velocity of light in a medium [see Eq. (14)]. We can see that this relationship is satisfied in the example considered here. However, in the case of pulses of shorter duration τ_p and longer cuvettes, we may find that the inequality (87) is not obeyed. In this case it is necessary to start from Eq. (14) [see next section].

It should be noted that Eq. (80) for the characteristic times Δt_m representing the time spent by a focal region at a given point in a medium, is valid only if the true velocity of foci v_{fm} is practically constant during the interval Δt_m. This condition is known to be violated at the turning point of the focal region, i.e., at t = 0. At these points the characteristic times $\Delta t_m^{(0)}$ are found from the condition $l_{fm}/2 = \zeta_{fm}(\Delta t_m^{(0)}/2) - \zeta_{fm}(0)$, which gives

$$\Delta t_m^{(0)} \approx \tau_p(N_{max}-N_m)\sqrt{\frac{l_{fm}}{N_{max}\chi_m k\bar{a}_0^2}}. \tag{88}$$

For the numerical example considered above Eq. (88) gives $\Delta t_m^{(0)} \approx 2 \times 10^{-9}$ sec. We can see that the value of $\Delta t_m^{(0)}$ representing the time spent by a focus at the turn-

ing point, is much shorter than the corresponding value of Δt_m in the exit plane of the medium $z = l$. Therefore, we may expect the processes occurring in matter at high energy densities and characterized by fairly long development times (for example, breakdown in a liquid) would appear first at the turning points of foci or close to them.[11] This explains the discrete nature of the optical breakdown in transparent dielectrics observed in[41] during the propagation of laser pulses.

We shall now estimate the total energy $W_m^{(0)}$ absorbed in a focal region during the characteristic turning time $\Delta t_m^{(0)}$ and the total energy W_m absorbed in the same region during the time Δt_m needed to cross the plane $z = l$. In general, we find that $W_m^{(0)} \sim P_{cr}^{(1)} \Delta t_m^{(0)}$ and $W_m \sim P_{cr}^{(1)} \Delta t_m$. For $P_{cr}^{(1)} \sim 20$ kW we find that under these conditions $W_m^{(0)} \sim 4 \times 10^{-5}$ J and $W_m \sim 2 \times 10^{-6}$ J. Depending on the actual absorption mechanism, some fraction of this energy may be used to heat the medium. If, for example, the stimulated Raman scattering is the main type of absorption, it follows that for $\omega_{-1}/\omega = 0.9-0.95$ a considerable part (90—95%) of the energy is transformed to the Stokes component and 5—10% is dissipated in the medium. We shall assume that 5% of the energy absorbed in a focal region is dissipated in heating the medium. Therefore, the temperature rise at a fixed point in carbon disulfide after the passage of a focal region should be $\Delta T^{(0)} \sim 100$ deg K at the turning point and $\Delta T \sim 5$ deg K at $z = l$. For other substances (toluene, nitrobenzene) the corresponding values of $\Delta T^{(0)}$ and ΔT are about one order of magnitude lower, for the same general conditions. Such local heating generates an acoustic wave, which results in the expansion of matter and a corresponding change (Δn_ρ) of the refractive index.[16] We can easily show that at the turning point of a focal region the calculated value of $|\Delta n_\rho|$ may exceed considerably $\Delta n = (1/2) n_0 n_2 |E_{fm}|^2$, obtained without allowance for the heating of the medium. This means that a multifocus structure cannot appear at all during the turning time of a focus or on approach to a turning point. On the other hand, in the case of rapidly moving foci (for example, in the $z \approx l$ plane) the influence of heating on a multifocus structure (or at least on the first foci) is unimportant ($|\Delta n_\rho| \ll \Delta n$) because the temperature rise is much lower and the time intervals Δt_m are much shorter. It should be noted that experimental observations of bright points on the end of a cuvette have established acoustic expansion of the substance after the appearance of these points.

A multifocus structure may disappear also because of the stimulated Raman scattering.[17] In fact, a stationary theory calculation of the gain experienced by the first Stokes component in the length of a focal region in the case of, for example, three-photon absorption (i.e., the calculation of the quantity $\exp[(4\pi\Gamma/\epsilon_0)(2\pi/\lambda_{-1})|E_{fm}|^2 l_{fm}]$ or—if Eqs. (72) and (74a) are used—of the quantity $\exp[(85\pi\Gamma/\epsilon_0)(\omega_{-1}/\omega)/n_2]$), gives $\sim e^{800}$ for carbon disulfide, $\sim e^{150}$ for toluene, and $\sim e^{70}$ for nitrobenzene (the values of Γ[48] are calculated using the absolute values of the Raman cross section and line width taken from[61,62]; the values of n_2 used for these substances are given in Footnote 14). These high calculated values of the gain indicate that such foci (their dimensions are governed by the instantaneous type of absorption) should not appear under stationary (steady-state) conditions because the energy of the beam would be transformed into the first Stokes component of the stimulated Raman scattering as a result of amplification of this spontaneously scatttered light.[18] This situation is possible at the calculated turning points of the foci or close to them. However, far from these points the stimulated Raman scattering becomes nonstationary (and therefore much less effective) if the foci move rapidly so that this type of scattering does not prevent the appearance of the foci. The stimulated Raman effect becomes nonstationary because in the case of large values of the gain the time needed for the establishment of steady-state conditions is much greater than the corresponding time for the establishment of the spontaneous Raman scattering as a result of the frequency dependence of the gain in the stimulated effect and anomalous dispersion of matter in the vicinity of the first Stokes frequency.[63,64] For example, the establishment time of the spontaneous Raman scattering in carbon disulfide is 2×10^{-11} sec.[62] For $\Delta t_m \sim 10^{-10}$ sec and a gain of the order of 800, it is clear that the stimulated Raman scattering in a focal region is far from stationary. Thus, the stimulated Raman effect may result in the disappearance (or a considerable increase in the dimensions) of a focus traveling between the exit plane of the medium and the calculated turning point. The moment at which such disappearance takes place is obviously governed by the condition that the absorption in the focal region due to the stimulated Raman effect becomes comparable with the instantaneous absorption such as that due to the three-photon mechanism. It is clear that at this moment an ultrashort pulse of the first Stokes component of the stimulated Raman effect will be excited[65] (for details see Sec. 3 in Chap. IV).

It should be noted that the disappearance of a multifocus structure as a result of turning of foci in nitrobenzene and carbon disulfide has been observed experimentally.[42] The disappearance of a moving focus on its approach to a calculated turning point in carbon disulfide and toluene has been observed in[51]. The influence of the stimulated Raman and Mandel'shtam-Brillouin scattering on the propagation of a beam between the entry plane of a nonlinear medium and the first focus has been considered in[44].

2 Propagation of short pulses

We shall now consider the propagation of laser pulses which are so short that the condition (87) is not satisfied. In this case we must start with Eq. (14) subject to the boundary condition (21). The introduction of a variable $t = \xi + (z/v)$ in Eq. (14) yields the following equation for E:

$$\Delta_\perp E + 2ik \frac{\partial E}{\partial z} + n_2 k^2 |E|^2 E = 0 \qquad (89)$$

subject to the boundary condition

$$E|_{z=0} = \varphi(r_\perp, \xi). \qquad (90)$$

This problem is again stationary and the variable ξ is simply a parameter in the boundary condition. Therefore, if we know the family of solutions of the problem (89)—(90) corresponding to all possible values of ξ, we can obtain the solution of the problem (14), (21) of interest to us by substituting $\xi = t - (z/v)$. In this way we obtain immediately a general conclusion that a multifocus structure of a light beam whose maximum power exceeds $P_{cr}^{(1)}$ appears also in those cases when the condition (87) is not satisfied. In such cases the general nature of the propagation of a beam is as follows. As under quasi-stationary conditions, the main feature of the propagation process is the appearance of moving foci on the

beam axis. In the case considered these foci appear at definite moments of time within a layer of a medium ($0 \leq z \leq l$), they split into pairs after appearance, and move along the z axis parallel and antiparallel to the direction of propagation of the incident beam.

a) Trajectories of foci.[51,66,67] We shall consider the specific case of an incident beam governed by the boundary condition (78). According to the above discussion, the positions of the foci ζ_{fm} along the z axis can be found by replacing t in Eq. (79) with $\xi = t - (\zeta_{fm}/v)$. This yields the following equation for ζ_{fm} at a given moment t:

$$\zeta_{fm} = \frac{\chi_m}{N_m} \frac{k\bar{a}_0^2}{\sqrt{P_0[t-(\zeta_{fm}/v)]/P_{cr}^{(m)} - 1}} . \quad (91)$$

However, it is more convenient to start discussion from a graphical method for the determination of the trajectories of the foci, which is equivalent to Eq. (91). In the graphical approach the coordinates $z/k\bar{a}_0^2$ and N are used to plot the dependences $N = N(z/k\bar{a}_0^2)$ represented by continuous curves in Fig. 10. This can be done using the curves given in Fig. 5 for weak absorption (Fig. 5 gives the converse dependence of $Nz/k\bar{a}_0^2$ on N). The same coordinates are used to plot the function

$$N = \frac{1}{E_{cr}} \left| E_0 \left(t - \frac{k\bar{a}_0^2}{v} \frac{z}{k\bar{a}_0^2} \right) \right|$$

represented by the dashed curve in Fig. 10. The values of $z/k\bar{a}_0^2$ corresponding to the points of intersection of the continuous and dashed curves give the positions (on a suitable scale) of the foci along the beam axis at a moment t. If we bear in mind that the dashed curve depends on time (this curve travels at a velocity $v/k\bar{a}_0^2$ along the axis $z/k\bar{a}_0^2$, remaining self-similar), we can easily determine the moments of appearance and the time dependences of the positions of the foci. The appropriate dependences are plotted in Fig. 11. We can see that the appearance of each focus is accompanied by its splitting into the pair. In this way, two groups of foci appear in the system. The group which travels parallel to the direction of propagation of the incident pulse is characterized by velocities which are always greater than the velocity of light v in the medium (they may even exceed the velocity of light in vacuum). This group of foci has no analog under quasistationary conditions. Each focus in the second group moves in the same way as under quasistationary conditions and its motion is first antiparallel to the incident beam and then such foci stop and turn back so that they finally travel parallel to the incident beam. The results of a quasistationary analysis are then obtained in the limit $l_t/l \to \infty$, where $l_t = \tau_p v$ is the length of a light train corresponding to the pulse duration τ_p and l is the thickness of the medium under investigation.

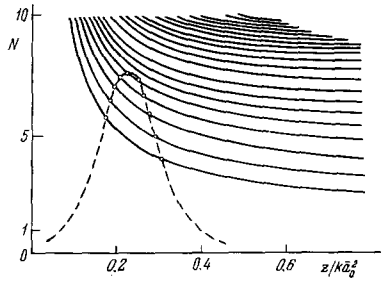

FIG. 10

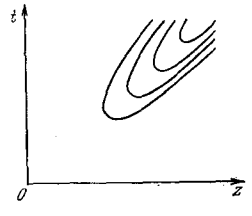

FIG. 11

We shall now consider in greater detail an incident pulse whose envelope is given by Eq. (82). It then follows from Eq. (91) that

$$t = \frac{\zeta_{fm}}{v} \pm \frac{\tau_p}{1.3} \sqrt{\frac{N_{max} - N_m - \chi_m (k\bar{a}_0^2/\zeta_{fm})}{N_m + \chi_m (k\bar{a}_0^2/\zeta_{fm})}} , \quad (92)$$

and hence the velocity of a focus $V_{fm} = d\zeta_{fm}/dt$ is given by

$$v_{fm} = \frac{vV_{fm}}{v + V_{fm}} , \quad (93)$$

where

$$V_{fm} = \pm \frac{\zeta_{fm}^2}{\chi_m k\bar{a}_0^2 N_{max}} \frac{2.6}{\tau_p} \left(N_{max} - N_m - \chi_m \frac{k\bar{a}_0^2}{\zeta_{fm}} \right)^{1/2} \left(N_m + \chi_m \frac{k\bar{a}_0^2}{\zeta_{fm}} \right)^{3/2}$$

is the corresponding value of the velocity of a focus under quasistationary conditions [see Eq. (86)]. For brevity, we shall call V_{fm} the quasistationary velocity.[19] It is clear from Fig. 11 that the points of appearance of the foci are found from the condition $dt/d\zeta_{fm} = 0$, which in combination with Eq. (93), yields

$$|V_{fm}| = v. \quad (94)$$

The solution ζ_{fm} of this equation can easily be obtained for several limiting cases. For example, if

$$\tilde{\zeta}_{fm} - \zeta_{min}^{(m)} \ll k\bar{a}_0^2, \ \zeta_{min}^{(m)} \quad (95)$$

the solution of this equation is

$$\tilde{\zeta}_{fm} = \zeta_{min}^{(m)} + \frac{(N_{max} - N_m)^2 (v\tau_p)^2}{(2.6)^2 N_{max} \chi_m k\bar{a}_0^2} . \quad (96)$$

It is also clear from Eq. (92) that the turning points of the foci $z = \zeta_{min}^{(m)}$ are described by the same expression as in the quasistationary case:

$$\zeta_{min}^{(m)} = \frac{\chi_m k\bar{a}_0^2}{N_{max} - N_m} . \quad (97)$$

The only difference is that now the turning moments $t^{(m)}$ of various foci are different:

$$t^{(m)} = \frac{\zeta_{min}^{(m)}}{v} . \quad (98)$$

According to Eq. (93), in the case of short pulses we may find that when a focus is sufficiently far from the boundary z = 0, its quasistationary velocity V_{fm} may exceed considerably the velocity of light in the medium:

$$V_{fm} \gg v. \quad (99)$$

In this case it follows from Eq. (93) that the true velocity of a focus v_{fm} is close to the velocity of light v.

b) Structure of moving foci. Since the variable $t = \xi + (z/v)$ substituted in Eq. (14) does not contain the transverse coordinate $\mathbf{r}_\perp$, the transverse structure of focal regions is the same as in the quasistationary case. On the other hand, the longitudinal structure is generally different. If we ignore the vicinities of the points where the foci appear $\tilde{\zeta}_{fm}$ and the turning points of the foci $\zeta_{min}^{(m)}$, these changes reduce to a change in the longitudinal scale, i.e., in the length of the focal regions. In this case we can use Eq. (69) and substituting $\zeta_{fm} = F_m\{[P_0[t - (z/v)]]\}$, we find that in the vicinity of the foci

$$|E|_{r=0}^2 = \begin{cases} \dfrac{|E_{fm}|^2}{\{1 + [(\Delta z - v_{fm}\Delta t)/(1 - (v_{fm}/v))\Lambda_{fm}|^2\}^\alpha}, & \dfrac{\Delta z - v_{fm}\Delta t}{1 - (v_{fm}/v)} < 0, \\ \dfrac{|E_{fm}|^2}{\{1 + [(\Delta z - v_{fm}\Delta t)/(1 - (v_{fm}/v))\Lambda_{fm}|^2\}^\beta}, & \dfrac{\Delta z - v_{fm}\Delta t}{1 - (v_{fm}/v)} > 0, \end{cases} \quad (100)$$

where $\Delta t = t - t_0$, $\Delta z = z - z_0$, and t_0 is the moment at which a focus crosses the plane z_0. It is clear from Eq. (100) as well as Eqs. (70) and (69) that in this case the

focal length $\tilde{l}_{fm}$ at a moment t_0 is related to the corresponding quasistationary value l_{fm} [see Eq. (74)] by

$$\tilde{l}_{fm}=\left|1-\frac{v_{fm}}{v}\right| l_{fm}. \tag{101}$$

The corresponding characteristic time $\Delta\tilde{t}_m$ during which a focal region remains at a given point z_0 is

$$\widetilde{\Delta t_m}=\frac{\tilde{l}_{fm}}{|v_{fm}|}=\left|1-\frac{v_{fm}}{v}\right|\frac{l_{fm}}{|v_{fm}|}. \tag{102}$$

We shall now consider the vicinity of the turning points of the foci. Using Eqs. (69), (83), and (98), we obtain by analogy with Eq. (100),

$$|E|^2_{r=0}=\begin{cases}\dfrac{|E_{fm}|^2}{[1+(\Delta/\Lambda_{fm})^2]^{\alpha}}, & \Delta<0,\\ \dfrac{|E_{fm}|^2}{[1+(\Delta/\Lambda_{fm})^2]^{\beta}}, & \Delta>0,\end{cases} \tag{103}$$

where

$$\Delta=\Delta z-\chi_m k\bar{a}_0^2\left(\frac{1.3}{\tau_p}\right)^2\frac{N_{max}[\Delta t-(\Delta z/v)]^2}{(N_{max}-N_m)^2},\qquad \Delta t=t-t^{(m)},\ \Delta z=z-\zeta^{(m)}_{min}. \tag{104}$$

It is clear from Eqs. (103) and (104) that the characteristic time $\widetilde{\Delta t}^{(0)}_m$ during which a focal region remains at a turning point is given by the same expression as under quasistationary conditions

$$\widetilde{\Delta t}^{(0)}_m=\Delta t^{(0)}_m\approx\tau_p(N_{max}-N_m)\sqrt{\frac{l_{fm}}{\chi_m k\bar{a}_0^2 N_{max}}}. \tag{105}$$

The longitudinal structure of focal regions considered at a fixed moment $t^{(m)}$ generally changes quite considerably. It follows from Eqs. (103) and (104) that this structure and the lengths of the focal regions remain the same as under quasistationary conditions ($\tilde{l}^{(0)}_{fm}=l^{(0)}_{fm}$) only if

$$v\Delta t^{(0)}_m\gg l_{fm}. \tag{106}$$

It follows directly from Eqs. (96) and (105) that if this condition is satisfied the turning point $\zeta^{(m)}_{min}$ and the point of appearance $\tilde{\zeta}_{fm}$ of the m-th focus are separated quite clearly ($\tilde{\zeta}_{fm}-\zeta^{(m)}_{min}\gg l_{fm}$). In the opposite case

$$v\Delta t^{(0)}_m\ll l_{fm} \tag{107}$$

these points merge in the sense that $\tilde{\zeta}_{fm}-\zeta^{(m)}_{min}\lesssim l_{fm}$. In this case Eq. (103) describes the vicinity of both points. It follows from Eqs. (103) and (104) that if the condition (107) is satisfied the dependence of $|E|^2_{r=0}$ on z at a moment $t^{(m)}$ has in this vicinity two maxima corresponding to the splitting of a focus into two components immediately after its appearance. The separation δ_m between these maxima is

$$\delta_m=\frac{(N_{max}-N_m)^2(v\tau_p)^2}{(1.3)^2N_{max}\chi_m k\bar{a}_0^2}, \tag{108}$$

i.e., it is four times as large as the distance $\tilde{\zeta}_{fm}-\zeta^{(m)}_{min}$ between the point of appearance to the turning point of a focus. If $v\Delta t^{(0)}_m\ll l_{fm}$, the minimum between these two maxima becomes very "shallow," i.e., at the moment $t^{(0)}_m$ the focus has not yet split into two components. In this case the total length of a focal region is

$$\tilde{l}^{(0)}_{fm}=v\Delta t^{(0)}_m. \tag{109}$$

We shall now consider a numerical example. We shall assume that the parameters of the beam are the same as in the first numerical example in Sec. 3 of Chap. III, i.e., we shall assume that $N_{max}=6$, $\bar{a}_0=0.15$ mm, $\lambda=0.5\times10^{-4}$ cm, $l_{fm}=0.1$ cm. We shall assume that the laser pulse duration is $\tau_p=3\times10^{-11}$ sec and we shall consider a layer of medium $l=10$ cm thick. It follows from Eqs. (93) and (59) that at $z=l$ the velocities of the foci are $v_{f1}\approx v_{f2}\approx v(1\pm2.6\times10^{-2})$ and $v_{f3}\approx(1\pm3.3\times10^{-2})$. We can see that in this plane the velocities of the foci are very close to the velocity of light v in the medium. In this case the longitudinal dimensions $\tilde{l}_{fm}$ of the moving foci are very small, $\tilde{l}_{fm}\approx3\times10^{-3}$ cm [Eq. (101)], and the times $\Delta\tilde{t}_m$ during which focal regions remain in this plane are $\Delta\tilde{t}_m\approx1.5\times10^{-13}$ sec [Eq. (102)]. The values of the corresponding times $\Delta\tilde{t}^{(0)}_m$ and dimensions $\tilde{l}^{(0)}_{fm}$ at the turning points of the foci, given by Eqs. (105), (107)—(109), are $\Delta\tilde{t}^{(0)}_m\approx3\times10^{-12}$ sec and $\tilde{l}^{(0)}_{fm}\sim0.1$ cm (since $v\Delta\tilde{t}^{(0)}_m\approx0.06$ cm $\sim l_{fm}$, the points of appearance of the foci merge with the turning points). It is interesting to note that in contrast to the quasistationary conditions, the length of each of the focal regions varies with time during the propagation of the light beam in the medium. It should also be noted that the times $\Delta\tilde{t}^{(0)}_m$ and $\Delta\tilde{t}_m$ are so short that the heating of the medium in the focal regions and its subsequent expansion during the passage of a pulse do not give rise to significant corrections in the refractive index. The corresponding expansion of matter and the associated change in the refractive index in the paths of the foci appear only after the end of the pulse.[20] It should also be noted that in the electron mechanism of the Kerr effect, when $\tau_K\lesssim10^{-15}$ sec, the conditions (9) of the validity of Eq. (14) are satisfied in the case considered above.

3. Excitation of ultrashort stimulated Raman scattering pulses

So far we have not considered specially the stimulated Raman scattering in the backward direction. However, attention has been drawn in[9] to the fact that under some conditions the backward effect may influence significantly some parts of the trajectories of moving foci. This influence appears in those cases when the point $\tilde{\zeta}_{fm}$ of appearance of a focus lies inside (or near the boundary) of a given layer of the medium and at the same time this point is well separated from the turning point $\tilde{\zeta}^{(m)}_{min}$. These conditions occur, for example, for the following parameters of the incident beam and the medium: $\bar{a}_0=0.15$ mm, $N_{max}=3.5$, $\lambda=0.5\times10^{-4}$ cm, $l_{fm}=0.1$ cm, $\tau_p=0.5\times10^{-8}$ sec, $l=30$ cm. It follows from Eqs. (85) and (59) that under these conditions there are only two foci (m = 1, 2) in the medium. Then, $\zeta^{(1)}_{min}\approx12$ cm, $\zeta^{(2)}_{min}\approx21$ cm. It also follows from Eq. (94) that the point of appearance of the first focus $\tilde{\zeta}_{f1}\approx26$ cm lies within the layer under consideration. Since $\tilde{\zeta}_{f1}-\zeta^{(m)}_{min}/l_{f1}\approx140$, the point of appearance of the first focus is well separated from its turning point. Between the point of appearance and the turning point the velocity of the first focus v_{f1} changes formally from $-\infty$ to 0 and at $z=z_{1v}\approx19$ cm this velocity becomes equal to v, i.e., to the velocity of light in the medium. At this point the light flux initially scattered spontaneously in the backward direction out of the focal region travels together with this region over a path Δz_{1v} which is generally given by the condition

$$\frac{v}{2}\frac{d^2t}{d\zeta^2_{fm}}\Big|_{\zeta_{fm}=z_{mv}}\left(\frac{\Delta z_{mv}}{2}\right)^2=\tilde{l}_{fm},$$

which, in combination with Eq. (92), gives

$$\Delta z_{mv}=\sqrt{\frac{2\tilde{l}_{fm}z_{mv}[N_{max}-N_m-\chi_m(k\bar{a}_0^2/z_{mv})][N_m+\chi_m(k\bar{a}_0^2/z_{mv})]}{N_m(N_{max}-N_m)+[(1/4)N_{max}-N_m]\chi_m(k\bar{a}_0^2/z_{mv})}}. \tag{110}$$

It follows from Eq. (110) that in the case under consider-

ation we have $\Delta z_{1v} \approx 1.5$ cm. Since $\Delta z_{1v}/\tilde{l}_{f1} \approx 8$, the total time of interaction of the focal region with the light flux scattered earlier has a sharp peak at the $z \approx z_{1v}$. Consequently, at $z \approx z_{1v}$ the energy of the focal region may be converted efficiently into the first Stokes component of the stimulated Raman scattering. The length of a light train of the first Stokes pulse should obviously be of the order of the length of the focal region $\tilde{l}_{fm}$ and, therefore, the duration of a pulse given by its transit across a fixed plane in the medium is of the order of $\tilde{l}_{fm}/v$. In the case considered we have $\tilde{l}_{fm}/v \approx 10^{-11}$ sec. An ultrashort stimulated Raman scattering pulse excited in this way still travels in the backward direction at the velocity of light in the medium. This pulse interacts with the remaining part of the light beam traveling in the opposite direction and the interaction amplifies further the Raman effect pulse and makes it highly directional. Such an interaction between two oppositely directed fluxes is described in[68,69]. The part of the original light beam which experiences this interaction may be so strongly suppressed that no further foci can appear. In this case the whole of that part of the trajectory of a focus which corresponds to $|v_{fm}| < v$ does not appear because of the backward stimulated Raman scattering. In Fig. 11 this region lies above the straight line $t = t_{mv} + [(z - z_{mv})/v]$, where t_{mv} is the moment when the focus crosses the plane z_{mv}.

Ultrashort pulses of the backward stimulated Raman scattering were observed experimentally for the first time in[68]. Attention was concentrated in[68,69] on the correlation between the appearance of these pulses and the formation of bright spots on the end of a cuvette containing the investigated substance. The above mechanism of the excitation inside a cuvette was proposed in[9]. An experimental confirmation of this mechanism of the excitation of ultrashort stimulated Raman effect pulses was confirmed experimentally in[9] on the basis of a correlation between these pulses and moving foci in the investigated medium. Ultrashort light pulses (of duration of the order of 10^{-11} sec) were also observed experimentally in the backward stimulated scattering in the wing of the Rayleigh line.[70,71] Clearly, the process of excitation and subsequent development of these pulses in the stimulated scattering in the wing of the Rayleigh line is analogous to the corresponding process in the stimulated Raman scattering.

We shall conclude this section by noting that if the excitation of ultrashort stimulated Raman effect pulses at $z = z_{mv}$ is not very effective because of the transient nature of the stimulated Raman effect, it follows from Eq. (5) that there is another possibility of formation of such pulses, which may be generated when the focal regions approach the turning points. As pointed out in Sec. 1 of Chap. IV, when a focus approaches a turning point the stimulated Raman scattering may at some time become sufficiently efficient for the total conversion of the energy in the focal region into the first Stokes component and this may produce ultrashort pulses of this component. If such conversion occurs in the immediate vicinity of a turning point, i.e., if $v_{fm} \ll v$, it is clear that the pulses of the first Stokes component should appear equally readily in the backward and forward directions. If the conversion time is sufficiently short, the duration of such pulses is of the order of $\tilde{l}_{fm}/v$. However, if the disappearance time of a focal region is longer than $\tilde{l}_{fm}/v$, the duration of a pulse governs the disappearance time of a focal region. The moment of disappearance of a focal region will be denoted by t_0 and the plane z in which this happens will be called z_0. In this case the interaction between the stimulated Raman effect pulses and the original light beam may suppress the parts of the trajectories of all the foci lying above the line $t = t_0 + [(z - z_0)/v]$ (see Fig. 11).[21)]

Ultrashort pulses of the first Stokes component were observed experimentally in[65] in a cuvette containing the investigated substance and they were found to travel in the forward and backward directions.

4. Broadening of the spectrum of pulses in a nonlinear medium

In the foregoing analysis we have been interested only in the distribution of the intensity $|E|^2$ of a light beam in a nonlinear medium. We shall now consider the total complex amplitude $E = |E|e^{i\varphi}$. This will allow us to study the spectral characteristics of a beam which has traversed a layer of the investigated medium. As before, we shall assume that the incident beam has a Gaussian distribution of the intensity in the transverse direction and an initially plane phase front, i.e., we shall assume that boundary condition at $z = 0$ is in the form of Eq. (78). We shall start from Eq. (14), i.e., we shall consider short pulses right from the beginning. According to the analysis in Sec. 2 of Chap. IV we must first write down the solution $E = E(r, z, E_0)$ of the corresponding stationary problem (21), (25). Then, the solution of the nonstationary problem of interest to us is given by the expression

$$\bar{E}(r, z, t) = E\left[r, z, E_0\left(t - \frac{z}{v}\right)\right]$$

For the sake of simplicity we shall consider only the field on the beam axis, i.e., we shall consider the region defined by $r = 0$, $z > 0$. It follows from Eqs. (25), (27), (30), and (31) that the solution $E(0, z, E_0)$ of the stationary problem is of the form

$$E(0, z, E_0) = |E(0, z, E_0)| \exp[i\varphi(0, z, E_0)], \qquad (111)$$

where

$$\varphi(0, z, E_0) = \int_0^z \left\{\frac{1}{2} n_2 |E(0, z', E_0)|^2 - [ka(z', E_0)]^{-2}\right\} dz',$$
$$a(z', E_0) = 1\Big/\sqrt{-\frac{\partial^2}{\partial r^2}\left|\frac{E(r, z', E_0)}{E(0, z', E_0)}\right|_{r=0}} \qquad (112)$$

is the "radius" of the beam defined for $r \to 0$. Equations (111) and (112) give the total complex amplitude E on the beam axis if we know the axial intensity ($|E|^2$) and the radius a of the intensity distribution in the paraxial region. We shall now employ Eqs. (111) and (112) in the analysis of the spectral properties of the beam.

a) Phase modulation of pulses. We shall begin with the case

$$z \ll k\bar{a}_0^2, \frac{\bar{a}_0}{\sqrt{n_2 E_{0\max}^2}}, \qquad (113)$$

where $E_{0\max}$ is the maximum value of E_0 during a pulse. In this case the solution of the stationary problem (21), (25) for $|E|^2$ gives [see, for example, Eqs. (42) and (43)]

$$|E(r, z', E_0)|^2 \approx E_0^2 e^{-r^2/\bar{a}_0^2}, \qquad (114)$$

and hence it follows from Eq. (112) that

$$\varphi(0, z, E_0) \approx kz\left[\frac{1}{2} n_2 E_0^2 - (k\bar{a}_0)^{-2}\right], \qquad (115)$$

and Eqs. (111) and (115) give the following expressions for $\bar{E}(r, z, t) = |\bar{E}|e^{i\bar{\varphi}}$:

$$|\bar{E}(0, z, t)| \approx \left|E_0\left(t-\frac{z}{v}\right)\right|, \quad (116a)$$

$$\bar{\varphi}(0, z, t) \approx \frac{1}{2} n_2 k z E_0^2\left(t-\frac{z}{v}\right) - \frac{z}{ka_0^2}. \quad (116b)$$

We can see that if the condition (113) is obeyed, the envelope of a pulse is propagated in the investigated nonlinear medium in the same way as in a linear medium. However, this is not true of the phase $\bar{\varphi}$. It follows from Eq. (116b) that in a nonlinear medium ($n_2 \neq 0$) the phase $\bar{\varphi}$ depends on time. It is modulated by the time dependence of the power of the incident beam in the entry plane of the medium. The depth of modulation of the phase is proportional to z, i.e., to the thickness of the nonlinear medium traversed by the pulse. The phase modulation alters the spectrum of the pulse traveling in the medium. The change in the spectrum can be determined by calculating directly the Fourier transform of the function $\bar{E}\exp(-i\omega_0 t)$; here, the exponential factor can be taken from Eq. (6) and for the sake of convenience we shall replace ω of Eq. (6) with ω_0. Such calculations are reported in[72] for pulses of different shapes. However, for the sake of brevity we shall consider only the calculation of the instantaneous frequency $\omega(t)$ of oscillations of the field in a given section z. It follows from Eq. (6) that we generally have $\omega(t) = \omega_0 + \Delta\omega(t)$, where

$$\Delta\omega(t) = -\frac{\partial\bar{\varphi}}{\partial t}, \quad (117)$$

For example, in the case of an envelope of a pulse given by Eq. (82), we find from Eqs. (116b) and (117) that

$$\Delta\omega(t) = 2kzn_2E_{0\max}^2\left(\frac{1.3}{\tau_p}\right)^2\left(t-\frac{z}{v}\right)\left\{1+\left[\frac{1.3(t-(z/v))}{\tau_p}\right]^2\right\}^{-3}. \quad (118)$$

The corresponding curve $\Delta\omega(t)$ is plotted in Fig. 12. We can see that $\Delta\omega(t)$ is an odd function of t relative to the point z/v and that it varies within the limits

$$\text{from } \Delta\omega_{\max} \approx (0.66/\tau_p)\, kzn_2E_{0\max}^2 \text{ to } \Delta\omega_{\min} = -\Delta\omega_{\max}.$$

The function $|\bar{E}(0, z, t)|$ is even with respect to the same point. Therefore, the spectral distribution of the intensity of oscillations of the electric field on the beam axis $I = |\bar{E}(0, z, \omega)|^2/\sqrt{8\pi}$, where

$$\bar{E}(0, z, \omega) = \int_{-\infty}^{\infty} \bar{E}(0, z, t)\, e^{-i(\omega_0-\omega)t}\, dt, \quad (119)$$

is symmetric relative to the frequency ω_0 and if $\Delta\omega_{\max} \gg 1/\tau_p$ the limiting frequencies are obviously $\omega = \Delta\omega_{\max}$ and $\Delta\omega_{\min}$. Consequently, the total width $\Delta\omega = \Delta\omega_{\max} - \Delta\omega_{\min}$ of the frequency distribution of the intensity I is given by[73]

$$\Delta\omega \approx \frac{1.3}{\tau_p} kzn_2E_{0\max}^2. \quad (120)$$

If we bear in mind that the width of the spectral distribution of the intensity of the incident beam is of the order of $1/\tau_p$, we find that Eq. (120) gives directly the broadening $\Delta\omega\tau_p$ of the spectrum during the propagation of the beam in a nonlinear medium. We can see that in the case of phase modulation the broadening of the spectrum is proportional to the path z traversed by the beam. We can also see that the broadening is proportional to the rate of change of the refractive index of the investigated substance ($n_2E_{0\max}^2/\tau_p$) and is thus of the Doppler type. The possibility of the Doppler broadening of the spectrum of a pulse which is traversed by a layer of a nonlinear medium was pointed out in[18]. Subsequently,[73] it was also mentioned that the same value of the instantaneous velocity $\omega(t)$ is obtained at two different moments t [see Eq. (118)]. If at these moments

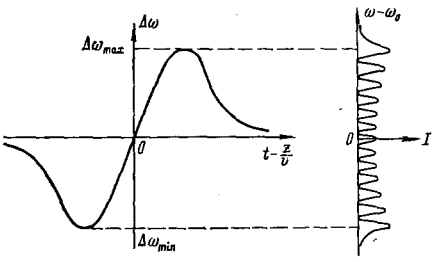

FIG. 12

the phase $\bar{\varphi}$ differs by $(2k+1)\pi$, where k is an integer, the distribution I clearly has a minimum near this instantaneous frequency. Similarly, if the phase difference is $2k\pi$, the distribution I has a maximum, i.e., the frequency distribution of the intensity I has a structure consisting of an oscillatory dependence of this quantity on ω with a large number of maxima and minima[73] (Fig. 12). We shall estimate the number of such extrema. According to Eq. (116b) the change in the phase $\bar{\varphi}$ during the time t from 0 to ∞ is $\Delta\bar{\varphi} = -kzn_2E_{0\max}^2$. Therefore, if $\Delta\omega \gg 1/\tau_p$, we have $|\Delta\bar{\varphi}| \gg 1$. The total (for $-\infty < \omega < \infty$) number of oscillations (for example, minima) is of the order of $\Delta\bar{\varphi}/2\pi \gg 1$ and the "average period" $\Delta\Omega$ of these oscillations is $\Delta\Omega = 2\pi\Delta\omega/|\Delta\bar{\varphi}| \approx 8/\tau_p$.

If the broadening of the pulse spectrum is sufficiently strong, the dispersion of the linear part of the refractive index n_0 may play an important role. This dispersion may disturb the phase relationships between the frequency components, i.e., a phase modulation may lead to an amplitude modulation. Beats between different frequency components may result in further broadening of the spectrum and this broadening can be described in the same way as in the case of beats between different components of a multimode laser beam. For example, the frequencies ω_L and $\omega_L - \omega_r$ may give rise to an anti-Stokes component $\omega_L + \omega_r$ and so on. This type of broadbroadening of the spectra of laser beams is discussed in[23,45]. It should also be noted that, as usual, the results given above are valid if the conditions (9) are satisfied. However, if for example, the condition (9b) is not obeyed, the spectral distribution of the intensity $I(\omega)$ becomes asymmetric with respect to the frequency ω_0.[74] If the conditions (9b) or (9c) are violated, the envelope of a pulse may change considerably during its propagation across a medium.[75] This also gives rise to an asymmetry in the spectrum $I(\omega)$ relative to the value of ω_0 with a stronger broadening on the energy scale in the Stokes region.[76]

b) Spectrum of a field of moving foci. We shall now consider the spectrum of a field E(t) in a fixed plane $z = z_0$ ($z_0 \neq \zeta_{fm}, \zeta_{min}^{(m)}$). This field is due to the passage of one of the moving focal regions across this plane [in this case Eq. (113) is not obeyed but the conditions (9) are satisfied]. The solution of the corresponding stationary problem for $|E|_{r=0}^2$ is now given by Eq. (69). The quantity $a(z', E_0)$ which appears in Eq. (112) can be estimated as follows. The power which flows through a section z in the vicinity of a focal region is $KP_{cr}^{(1)}$. The coefficient K is of the order of unity and it decreases with increasing z: for example, if $\zeta_{fm} - z \ll l_{fm}$ we have $K \approx 1$ but if $z = \zeta_{fm}$ we have $K \approx 2/3$. Bearing in mind that the transverse distribution of the intensity in the vicinity of a focus is nearly Gaussian [see Eq. (69)], we find that $(1/2)n_2|E(0, z', E_0)|^2 = 2K(z')[ka(z', E_0)]^{-2}$.

In order to explain the main features of the spectrum of a field of moving foci, we shall assume for simplicity that $K(z') \equiv 1$ and that $\alpha = \beta = 1$ in Eq. (69), i.e., we shall confine ourselves to the approximate dependence of $|E|^2$ in the vicinity of a focus, which is symmetric with respect to the point ζ_{fm}. It then follows from Eqs. (111) and (112) that

$$E(0, z, E_0) = \frac{|E_{fm}| \exp(i\chi_0)}{\sqrt{1+\{[z-\zeta_{fm}(E_0)]/\Lambda_{fm}\}^2}} \times \exp\left[\frac{i}{4} k\Lambda_{fm} n_2 |E_{fm}|^2 \operatorname{arctg}\left(\frac{z-\zeta_{fm}(E_0)}{\Lambda_{fm}}\right)\right], \quad (121)$$

where χ_0 is a constant and the value of $\overline{E}$ at the time close to the moment t_0 when a focal region crosses the plane z_0 is given by

$$\overline{E}(0, z_0, t) = \frac{|E_{fm}| \Delta t_x \exp(i\chi_0)}{\sqrt{(\Delta t_x)^2 + (t-t_0)^2}} \left[\frac{\Delta t_x + i(t-t_0)}{\Delta t_x - i(t-t_0)}\right]^{\alpha/2}, \quad (122)$$

where

$$\Delta t_x = \frac{\Lambda_{fm}}{|V_{fm}|}, \quad \alpha = \frac{(-1)^s}{4} k\Lambda_{fm} n_2 |E_{fm}|^2 \quad (s = 0, 1). \quad (123)$$

where V_{fm} is the quasistationary velocity of a focus in the plane z_0; $s = 0$ for $V_{fm} < 0$ and $s = 1$ for $V_{fm} > 0$.

The Fourier transform (119) of the function (112) is[77]

$$\overline{E}(0, z_0, \omega) = \begin{cases} -\frac{F \exp[i(\omega-\omega_0)t_0]}{\sqrt{\omega_0-\omega}\,\Gamma\left(\frac{\alpha+1}{2}\right)} W_{\alpha/2, 0}[2\Delta t_x(\omega_0-\omega)] & (\omega < \omega_0), \\ \frac{F \exp[i(\omega-\omega_0)t_0]}{\sqrt{\omega-\omega_0}\,\Gamma\left(\frac{1-\alpha}{2}\right)} W_{-\alpha/2, 0}[2\Delta t_x(\omega-\omega_0)] & (\omega > \omega_0), \end{cases} \quad (124)$$

where $F = \pi E_{fm}\sqrt{2\Delta t_x}\exp(i\chi_0)$; $\Gamma(z)$ is the gamma function; $W_{\lambda,\mu}(z)$ is the Whittaker function. The value of α in the above expression can easily be estimated using Eqs. (70), (72), and (74). For example, in the three-photon absorption case we have $|\alpha| \approx 2$. It follows from Eq. (124) with $|\alpha| = 2$ that the spectral distribution of the intensity is asymmetric with respect to the point $\omega = \omega_0$. If $V_{fm} < 0$, a great proportion of the energy is located on the $\omega < \omega_0$ side, i.e., the spectrum broadens preferentially into the Stokes region. In the opposite case, when $V_{fm} > 0$, the greater proportion of the energy is located on the $\omega > \omega_0$ side, i.e., in the anti-Stokes region. In both cases the total width of the spectrum $\Delta\omega$ of a moving focus is[22)]

$$\Delta\omega \approx \frac{\omega_0}{2} \frac{|V_{fm}|}{c} \Delta n_{fm}, \quad (125a)$$

where $\Delta n_{fm} = (1/2) n_0 n_2 |E_{fm}|^2$ is the increase in the refractive index at the point where the energy density has its highest value in a given focal region. Eqs. (125a) and (72) can be written in the form

$$\Delta\omega \approx 0.3 |V_{fm}| \frac{\lambda}{d_{fm}^2}. \quad (125b)$$

It should be noted that the quasistationary velocity of a focus V_{fm} which occurs in Eq. (125a) and (125b) is equal to the true velocity of a focus v_{fm} only under quasistationary conditions. In the general case of short pulses we can use Eq. (93) to express the quasistationary velocity in terms of v_{fm}:

$$V_{fm} = \frac{v v_{fm}}{v - v_{fm}}. \quad (125c)$$

The expression (125a) was obtained in[77] and it is equivalent to the expression given in[78] subject to the condition (125c).

It follows from Eqs. (123)—(125) that in the part of the trajectory of a focus corresponding to $-\infty < v_{fm} < 0$ the broadening of the spectrum is mainly in the direction of the Stokes region. If $0 < v_{fm} < v$, the spectrum broadens mainly into the anti-Stokes region. Finally, if $v_{fm} > v$ the spectrum broadens more strongly, as pointed pointed out in[78], into the Stokes region. It is also clear from Eqs. (125a)—(125c) that under quasistationary conditions the width of the spectrum $\Delta\omega$ is proportional to the velocity of a focus v_{fm} and, therefore, for constant values of $|E_{fm}|^2$, this width increases monotonically with increasing distance from the turning point of this focus to the plane under consideration (z_0).[23)] In the case of short pulses the width $\Delta\omega$ resulting from the motion of a focus also increases with the distance z_0 from the entry plane of the medium because $(v_{fm} - v)/v$ tends to zero for $z_0 \to \infty$. It is clear that under real conditions this rise occurs as long as $|E_{fm}|^2$ remains constant. In general, we must bear in mind that in the corresponding stationary case of the first (and any other) focus we have $N \to N_1$ for $z_0 \to \infty$; on the other hand, in the case of $N \to N_1$ and a fixed value of the nonlinear (for example three-photon) absorption coefficient m_4 the value of $|E_{fm}|^2$ is practically constant only in a restricted range of values of z_0 whereas over a wide range of z_0 measured from the entry plane of the medium this quantity decreases rapidly with increasing distance. This implies the disappearance of the foci.[24)] In the experimental investigations[39,52] carried out on giant pulses it has been established that the disappearance of the bright points on the end of a cuvette occurs if the cuvette length is of the order of 50—100 cm.

We shall now estimate the width of the spectrum $\Delta\omega$ of moving foci in a number of cases. In the numerical example considered in Sec. 1 of Chap. IV ($\tau_p = 2 \times 10^{-8}$ sec) we obtain $\Delta\omega \approx 0.3$ cm^{-1}. This value is in agreement with an estimate of $\Delta\omega$ obtained by direct measurements in[51] under similar conditions (the value of $\Delta\omega$ found experimentally in[51] does not exceed 1 cm^{-1}). In the numerical example considered in Sec. 2b of Chap. IV ($\tau_p = 3 \times 10^{-11}$ sec) we find that $\Delta\omega \approx 200$ cm^{-1}. If in the same example we assume that the laser pulse duration is 3×10^{-12} sec, we find that $\overline{\gamma}_{fm} \approx 3 \times 10^{-4}$ cm $\sim d_{fm}$, i.e., strictly speaking one of the conditions of Eq. (9b) is violated. However, this does not affect the estimate of the value of $\Delta\omega$ which is ≈ 2000 cm^{-1}. These values are in agreement with the widths found experimentally in[29,80,81] for laser pulses of 10^{-11}—3×10^{-12} sec duration. Finally, if $d_{fm} = 10^{-4}$ cm (this is of the order of magnitude of the transverse size of bright spots in several glasses) and $\tau_p = 3 \times 10^{-12}$ sec, it follows from Eq. (125) that $\Delta\omega \approx 5 \times 10^4$ cm^{-1}. This value is greater than the laser frequency $\omega_0 \approx 14\,000$ cm^{-1}, i.e., we may expect superbroadening of the spectrum of the incident pulse. Such superbroadening has been observed experimentally[82] in glasses for laser pulses of about 3×10^{-12} sec duration.

It should be pointed out that for values of $\Delta\omega$ as large as 10^3—10^4 cm^{-1} a detailed description of the spectrum of the field of moving focal regions may have to include an allowance for the dispersion of the linear part of the refractive index. However, this problem has not yet been tackled.

It should be noted also that the interference between the spectra of two (or a larger number) of focal regions may give rise to a quasiperiodic structure in the overall frequency distribution of the intensity. The period $\Delta\Omega$ of this structure is $\Delta\Omega \approx \pi/\Delta t$ where $\Delta t = t_m - t_n$ is the interval between the moments when a given section z_0

is crossed by the focal regions under investigation. Depending on the experimental conditions, the spectral distribution may be of the continuous type[83,84] or it may have a quasiperiodic structure.[73,74,83,84]

V. CONCLUSIONS

We have considered the characteristic features of the propagation of high-power light beams in media with the Kerr nonlinearity when the conditions (9) are satisfied (these conditions are of greatest practical interest). One of the consequences of the theory developed above is that under typical conditions the diameters of the foci are practically independent of the incident beam power and of the duration of laser pulses. This is the situation observed experimentally for giant and ultrashort (picosecond) laser pulses. This allows us to assume that the conditions (9) are satisfied under real conditions not only by giant but also by picosecond pulses and, therefore, the Kerr effect, like the nonlinear absorption of the medium, is governed by some rapid-response mechanism.

1. Generalizations of the theory

We shall now consider the question of the propagation of light beams in a medium when the conditions (9) are not satisfied. We shall start by noting that recently several workers (see, for example,[45,52]) have considered the case when the condition (9d) is not satisfied, i.e., when the inertia of the Kerr effect is considerable. This may occur, for example, in the case of picosecond laser pulses if the main nonlinearity mechanism is the orientational Kerr effect. In general, we must distinguish two possible variants. In the first variant the inertia of the Kerr effect does not influence the formation of foci and is manifested only in a focal region. Then, the dimensions of a focal region are governed by the finite establishment time of the Kerr effect. Since the process under consideration is more sensitive to the change in the imaginary part of the refractive index than to the real part, the direct cause of the limitation of the intensity in a focus may be the nonlinear absorption associated with the delay (inertia) of the polarization response of the medium to an electric field. Therefore, under these conditions we may expect a multifocus structure of a light beam similar to that considered in Sec. 2 of Chap. III. In the second variant the inertia of the Kerr effect has a strong influence on all parts of a beam in a medium. The relevant solution can be obtained numerically (the published attempts to solve problems analytically are based on the assumption of retention of a Gaussian distribution of the intensity in a beam and, therefore, are not sufficiently reliable; see Sec. 2 in Chap. II). The results of a numerical solution of this problem are given in[85] but a complete solution of all aspects of the propagation of the beam has yet to be obtained. It is simply concluded in[85] that the waveguide regime is not predicted by their solution.

It should be noted from the theoretical point of view that the diameters of filaments (trajectories of foci) should depend in both variants on the observational conditions (power of the beam, duration and shape of laser pulses) but this has yet to be confirmed experimentally and, therefore, we may assume that the inertia of the Kerr effect is absent under the conditions considered. Therefore, we shall not discuss this point in greater detail.

We shall now consider the case when the nonlinear absorption in a medium is very weak so that the conditions (9a)—(9c) are not satisfied in a focal region. According to the theory presented above, under typical conditions these inequalities contain only one independent small parameter, for example, $\lambda/\Lambda_\perp$ and their violation means that $\Lambda_\perp \sim \lambda$. In this case the propagation of a beam can be described directly by the Maxwell equations which predict the appearance of a wave reflected from the point of collapse z^* (see Sec. 3 of Chap. II and Sec. 2 of Chap. III) backward or at a large angle with respect to the beam axis. In the case of a wave which travels forward across the point of collapse, this reflection is equivalent to a nonlinear absorption which appears only if the transverse dimensions are of the order of λ. Therefore, we may expect a multifocus structure in a light beam similar to that considered in Sec. 2 of Chap. III and the absence of the true nonlinear absorption in the medium.

Under some special conditions (for example, in the case of significant ionization of matter in a focal region) the main intensity-limitation mechanism may be a weakening of the nonlinearity of the real part of the refractive index n because of the appearance of free electrons. Strictly speaking, under such conditions the dependence of the real part of the refractive index on the intensity of light ($|E|^2$) can be represented only in the form of a functional. Numerical calculations on a computer (for the existing memory access times and computation rates) present a daunting problem even when the parabolic equation can be used. Therefore, as a rough model it would be interesting to discuss a medium with a refractive index n depending on $|E|^2$ in the form of a suitable function such as Eq. (17), in the form of a saturable Kerr nonlinearity (it is understood that the value of $|E_s|^2$ is artificially reduced). Numerical calculations[86] based on the parabolic equation show that the model of a saturable Kerr nonlinearity leads to a multifocus structure in a light beam even without allowance for the nonlinear absorption if $P > P_{cr}^{(1)}$, $|E_{f1}|^2 \gtrsim 100$ (see Sec. 3 in Chap. III). In this case the structure of the foci can be described by Eqs. (67)—(69) in which we have to simply substitute $\beta \approx \alpha$.

2. Experimental results

We shall now consider briefly the results of experimental investigations of the propagation of high-power laser beams in matter. The formulation of the moving foci theory[11] was followed by several experimental investigations intended to determine whether moving foci or waveguide filaments are actually observed (the waveguide filaments are discussed in the Introduction in Chap. I). It was established in[51,42,43,52,9,87,88] that moving foci are observed in the propagation of giant laser pulses. Direct photographs of the trajectories of foci in a multifocus structure were obtained in[42] by high-speed time scanning. A stationary (steady-state) multifocus structure was observed in[43]. Foci moving at a velocity higher than that of light were reported in[52] (the relevant theory is presented in Sec. 2 of Chap. IV). A good quantitative agreement between the theoretical and experimental values of the distance between a moving focus and an ultrashort backward stimulated Raman scattering pulse was obtained in[9] at different moments and for a wide range of incident pulse powers. The diameters of focal regions in benzene solu-

tions were investigated in[87] and comparison of the theoretical and experimental values indicated that the main energy-density-limiting mechanism in the focal regions was the stimulated Raman scattering in the forward direction (in agreement with the theory given in Sec. 2b of Chap. III). A good quantitative agreement was established in[88] between the experimentally obtained values of the broadening of the spectrum and the corresponding theoretical values [see Eq. (125)] and this agreement was obtained for different cuvette lengths and incident pulse powers.

A recent attempt[89] to detect a waveguide filament failed to give positive results. An earlier report[90] of waveguide filaments was in error because the length (~ 10 cm) of a "filament" observed in[90] did not exceed the length $l_f = 0.7kd^2 = 1.4\pi d^2/\lambda$ (see Footnote 13) of a focal region in a Gaussian beam in a linear medium; this length was deduced from the "filament" diameter $d = (1-1.5) \times 10^{-2}$ cm ($\lambda \approx 0.5 \times 10^{-4}$ cm) determined experimentally in[90].

According to the theory given above (see Sec. 2 in Chap. IV) a multifocus structure should also appear in picosecond laser pulses at least if the Kerr effect mechanism is sufficiently fast (for example, in the case of the electron mechanism). It should be noted that for bright spots of $d \sim 10^{-3}$ cm typical diameter the corresponding length of a focal region in a linear medium l_f is 10^{-1} cm even in the case of a Gaussian beam, i.e., it is of the order of the total length of a light train corresponding to a typical pulse duration $\tau_p \sim 3 \times 10^{-12}$ sec. Therefore, waveguide filaments cannot form under these conditions.

We shall now consider briefly the experimental investigations of the propagation of picosecond laser pulses in matter. Bright spots on the endof a cuvette during the propagation of such pulses were first reported in[24]. Later, the results obtained in the study of the broadening of the spectra were used to draw the conclusion[80] that a thin core with a high energy density formed in a light train and this core had a smooth longitudinal intensity distribution and its length was of the order of the total light train. A similar pattern was described as a model in earlier papers.[13,14] However, it seems to us that the results reported in[80] can be explained by assuming the appearance of a multifocus structure. In a later paper[81] the same authors come round to the conclusion that a moving focus is formed under these conditions.

Recently Korobkin[91] and others observed bright spots on the sides of a cuvette filled with a liquid dielectric and illuminated with picosecond pulses. The positions of these spots were in good agreement with the theoretically predicted turning (stopping) points of foci in a multifocus structure [see Eq. (97)]. The discrete nature of the observed pattern can be explained by the fact that the focal regions spend the longest time at the turning points and, therefore, these points are the brightest (see Sec. 1 in Chap. IV). It is concluded in[91] that a multifocus structure is observed.

Thus, in the case of giant laser pulses the theory of multifocus structure and moving foci has been fully confirmed in experimental investigations. In the case of picosecond laser pulses the first experimental data support the theory.

[1)] We must make the stipulation that generally speaking the Kerr effect is governed by the nature of the nonlinearity of the medium in the case of nonresonant interactions of light with matter. A different type of nonlinearity appears in the special case of resonant interactions such as those which occur in gases when the frequency of light is close to one of the frequencies of molecular or atomic transitions. The propagation of light pulses under such resonant conditions is outside the scope of the present review. Such a review is given in [1].

[2)] It is pointed out also in [27,28] that the Kerr effect may also arise as a result of a fast-response mechanism associated with "librational" molecular vibrations. A fast-respnse mechanism representing "microscopic grouping" of molecules is discussed in [29].

[3)] This parabolic equation has been used for a long time in descriptions of wave processes in linear media. In a linear weakly inhomogeneous medium it has the form of Eq. (10), where $\delta\epsilon = \delta\epsilon(\mathbf{r}, t)$.

[4)] The dependence of the refractive index of a medium on the intensity of light in the transient case when the condition (9b) is not satisfied is also discussed in [17].

[5)] However, this point is ignored in several papers (see, for example, [30-32]) which deal with the propagation of light beams on the basis of the parabolic equation in the case when the Kerr nonlinearity of the medium is saturated significantly.

[6)] In the opposite case $n_2 |E|^2 \geqslant 1$, it follows from Eq. (9) that $\Lambda \leqslant \lambda/2$. Therefore, the description of the propagation of light beams in nonlinear media allowing only for the saturation of the Kerr effect (when $n_2 |E|^2 \geqslant 1$) would have required—even in the stationary case—the direct use of the Maxwell equations rather than the parabolic equation.

[7)] The conditions (9c), (9d), and (19) of the validity of Eq. (20), associated with the variation of alight beam with time, will be considered later (see Sec. 1 of Chap. IV).

[8)] This also applies to a beam which has been focused by an ordinary lens and obeys the boundary condition of Eq. (36). The numerical solution of this case is given in [46]. It should also be noted that a similar problem has been considered in [47]. However, the transformation of variables used in the latter paper gives rise to a discontinuity in the solution at $z = R$, i.e., in the focal plane of the lens. Therefore, the propagation of a beam predicted in [47] for the $z > R$ range is incorrect.

[9)] It is only worth noting that there is an experimental investigation [49] which suggest that the process is possible.

[10)] The role of the excited vibrational states of molecules is considered in [39,50].

[11)] As in Sec. 3 in Chap. II, we shall not consider the existence of a mathematical singularity in this solution but we shall simply assume that the steepness of the rise of $|X|^2$ with z on approach to the first focus is sufficiently high to violate the condition of validity of the initial equation (60) given by $\Lambda_{\|} \gg \lambda$ [see Eq. (9)].

[12)] It should be noted that according to Eq. (73a), the inequality $\delta\epsilon'' \ll \delta\epsilon'$ is satisfied in the focal region and, consequently, throughout the medium. As mentioned in Sec. 1 of Chap. II, this allows us to ignore the corrections to the real part of ϵ associated with the presence of $\delta\epsilon''$. Direct numerical calculations including these corrections [$\delta\epsilon$ is expressed in the form $\delta\epsilon = (1/2)\epsilon_2 |E|^2 - \epsilon_0 n_4 |E|^4 + i\epsilon_0 m_4 |E|^4$, where $n_4 \ll m_4$] show that the beam propagation is basically unchanged. Quantitative changes in the propagation process are small. For example, the changes in the diameter of the focal regions do not exceed 15%.

[13)] For example, it follows from Eq. (34) that in the case of focusing of a Gaussian beam in a linear medium the corresponding length of $l_f \approx 0.7 \times kd_1^2$. The expressions for beams with non-Gaussian distributions of the intensity the expression is the same except for the numerical coefficient.

[14)] The value of P_{cr} for carbon disulfide was determined experimentally in [53]. The experimental values of P_{cr} for toluene and nitrobenzene were found in [54] to be 55 and 19 kW, respectively, and the values of n_2 for these substances were approximately 0.2×10^{-11} and 0.5×10^{-11} cgs esu.

[15)] A theoretical discussion of two-dimensional beams in nonlinear media of the type considered here [57] is of formal naturé because under real conditions such beams split into three-dimensional components which may be close to axial symmetry.

[16)] It should be noted that because under normal conditions the velocity of foci is supersonic, the perturbations of the density in the medium are concentrated in an acoustic cone. In general, these perturbations include a contribution not only of heating but also of electrostriction in a focal region.

[17)] A similar influence may sometimes be exerted by the stimulated Mandel'shtam-Brillouin scattering, stimulated scattering in the wing of the Rayleigh line, and so on.

[18)] According to the results given in Sec. 2b of Chap. III, the gain from which the stationary (quasistationary) stimulated Raman scattering be-

gins to suppress the foci (starting from the first) can be found from the condition $H_{cr} \approx N$ (or, which is equivalent, $4\pi\Gamma/\epsilon_0 \approx n_2$). We can see that for the conditions assumed in Sec. 2b of Chap. III this amounts to only $\sim e^{20}$, i.e., gain is now much smaller than the values given above. It should be noted that in the case of carbon disulfide the gain in a focal region under stationary conditions is in fact much less than e^{800} as a result of strong excitation of the upper vibrational states of molecules in the stimulated Raman scattering. However, this reduction in the gain is relatively small and does not play the dominant role in the effect discussed here.

[19)] We can easily show the relationship (93) between the true velocity of a focus v_{fm} and the corresponding quasistationary velocity V_{fm} applies for any approximation of the position of the foci as a function of the initial power $\zeta_{fm} = F_m(P_0)$ [see, for example, Eq. (58)] in the corresponding stationary problem and for any envelope of a laser pulse $P_0(t)$ [see, for example Eq. (82)]. Obviously, under quasistationary conditions we have $v_{fm} \approx V_{fm}$.

[20)] This is easily demonstrated if we bear in mind that the total energy $\tilde{W}_m$ absorbed in the volume occupied by a focal region during the transit of this region across a fixed section $z \neq \zeta_{min}^{(m)}$, ζ_{fm} is of the order of $P_{cr}^{(1)} \tilde{l}_{fm} \widetilde{\Delta t_m} / \tilde{l}_{fm}$, and, similarly, for $z = \zeta_{min}^{(m)}$ the corresponding energy $W_m^{(0)}$ is of the order of $P_{cr}^{(1)} \tilde{l}_{fm}^{(0)} \widetilde{\Delta t_m}^{(0)} / l_{fm}$.

[21)] We must point out that this conclusion applies only to sufficiently short laser pulses. In the opposite case of quasistationary light beams the stimulated Raman scattering pulses escape from the nonlinear layer in a time much shorter than the duration of a laser pulse and this means that new parts of this pulse may be focused subsequently. The slope of the leading edge of a new part of a laser pulse obviously corresponds to the duration of an ultrashort stimulated Raman scattering pulse. Thus, the time scale of the change in the intensity of the incident beam may be equal to the duration of ultrashort pulses even in the case of giant laser pulses. This may have a considerable influence on the spectral properties of the field of moving foci (see Sec. 4 in Chap. IV).

[22)] We can easily show that this expression represents the total integral of the variation of the instantaneous frequency $\omega(t)$ of the field E at the point z_0.

[23)] These results are not in agreement with the theoretical conclusions reached in [79], where it is assumed that the width of the spectrum $\Delta\omega$ of a moving focal region has a *maximum* located between a turning point and the exit plane of the medium at a distance equal to the longitudinal size l_{fm} of the focal region measured from the turning point.

[24)] In contrast to the disappearance of the foci discussed in Secs. 1 and 3 in Chap. IV, which is due to the expansion of the substance or to the stimulated scattering, in the present case the disappearance is due to the fastest and spatially local nonlinear absorption mechanism.

[1] G. L. Lamb Jr., Rev. Mod. Phys. **43**, 99 (1971).
[2] R. Y. Chiao, E. Garmire, and C. H. Townes, Phys. Rev. Lett. **13**, 479 (1964).
[3] P. L. Kelley, Phys. Rev. Lett. **15**, 1005 (1965).
[4] T. F. Volkov, Sbornik "Fizika plazmy i problema upravlyaemych termoyadernykh reaktsii," (Collection: Physics of Plasma and Problem of Controlled Thermonuclear Reactions), Vol. III, Atomizdat, M. (1958), p. 336.
[5] G. A. Askar'yan, Zh. Eksp. Teor. Fiz. **42**, 1567 (1962) [Sov. Phys.-JETP **15**, 1088 (1962)].
[6] V. I. Talanov, Izv. Vyssh. Ucheb. Zaved., Radiofiz. **7**, 564 (1964).
[7] A. Szöke, Bull. Amer. Phys. Soc. **9**, 490 (1964).
[8] V. N. Lugovoĭ and L. I. Sobel'man, Zh. Eksp. Teor. Fiz. **58**, 1283 (1970) [Sov. Phys.-JETP **31**, 690 (1970)].
[9] M. M. T. Loy and Y. R. Shen, Appl. Phys. Lett. **19**, 285 (1971).
[10] A. L. Dyshko, V. N. Lugovoĭ, and A. M. Prokhorov, ZhETF Pis. Red. **6**, 655 (1976) [JETP Lett. **6**, 146 (1967)].
[11] V. N. Lugovoĭ and A. M. Prokhorov, ZhETF Pis. Red. **7**, 153 (1968) [JETP Lett. **7**, 117 (1968)].
[12] A. L. Dyshko, V. N. Lugovoĭ, and A. M. Prokhorov, Zh. Eksp. Teor. Fiz. **61**, 2305 (1971) [Sov. Phys.-JETP **34**, 1235 (1972)].
[13] S. A. Akhmanov, A. P. Sukhorukov, and R. V. Khokhlov, Zh. Eksp. Teor. Fiz. **50**, 1537 (1966) [Sov. Phys.-JETP **23**, 1025 (1966)].
[14] S. A. Akhmanov, A. P. Sukhorukov, and R. V. Khokhlov, Usp. Fiz. Nauk **93**, 19 (1967) [Sov. Phys.-Uspekhi **10**, 609 (1968)].
[15] R. G. Brewer, J. R. Lifsitz, E. Garmire, R. Y. Chiao, and C. H. Townes, Phys. Rev. **166**, 326 (1968).
[16] T. K. Gustafson, P. L. Kelley, R. Y. Chiao, and R. G. Brewer, Appl. Phys. Lett. **12**, 165 (1968).
[17] T. K. Gustafson and C. H. Townes, Phys. Rev. **A6**, 1659 (1972).
[18] Ya. B. Zel'dovich and Yu. P. Raĭzer, ZhETF Pis. Red. **3**, 137 (1966) [JETP Lett. **3**, 86 (1966)].
[19] Y. R. Shen, Phys. Lett. **20**, 378 (1966).
[20] Y. R. Shen and Y. J. Shaham, Phys. Rev. **163**, 224 (1967).
[21] Yu. P. Raĭzer, Zh. Eksp. Teor. Fiz. **52**, 470 (1967) [Sov. Phys.-JETP **25**, 308 (1967)].
[22] P. Lallemand and N. Bloembergen, Phys. Rev. Lett. **15**, 1010 (1965).
[23] N. Bloembergen and P. Lallemand, Phys. Rev. Lett. **16**, 81 (1966).
[24] R. G. Brewer and C. H. Lee, Phys. Rev. Lett. **21**, 267 (1968).
[25] M. A. Duguay, J. W. Hansen, and S. L. Shapiro, IEEE J. Quantum Electron. **QE-6**, 725 (1970).
[26] R. W. Hellwarth, A. Owyoung, and N. George, Phys. Rev. **A4**, 2342 (1971).
[27] I. L. Fabelinski and V. S. Starunov, Appl. Opt. **6**, 1793 (1967).
[28] R. Polloni, C. A. Sacchi, and O. Svelto, Phys. Rev. Lett. **23**, 690 (1969).
[29] R. W. Hellwarth, Phys. Rev. **152**, 156 (1966).
[30] J. H. Marburger and E. Dawes, Phys. Rev. Lett. **21**, 556 (1968).
[31] E. L. Dawes and J. H. Marburger, Phys. Rev. **179**, 862 (1969).
[32] V. E. Zakharov, V. V. Sobolev, and V. S. Synakh, Zh. Eksp. Teor. Fiz. **60**, 136 (1971) [Sov. Phys.-JETP **33**, 77 (1971)].
[33] V. N. Lugovoĭ, Dokl. Akad. Nauk SSSR **176**, 58 (1967) [Sov. Phys.-Doklady **12**, 866 (1968)].
[34] V. I. Talanov, ZhETF Pis. Red. **2**, 218 (1965) [JETP Lett. **2**, 138 (1965)].
[35] E. L. Kerr, Phys. Rev. **A4**, 1195 (1971).
[36] V. N. Gol'dberg, V. I. Talanov, and R. É. Érm, Izv. Vyssh. Ucheb. Zaved., Radiofiz. **10**, 674 (1967).
[37] Y. R. Shen and Y. J. Shaham, Phys. Rev. Lett. **15**, 1008 (1965).
[38] R. G. Brewer and J. R. Lifsitz, Phys. Lett. **23**, 79 (1966).
[39] R. Y. Chiao, M. A. Johnson, S. Krinsky, H. A. Smith, C. H. Townes, and E. Garmire, IEEE J. Quantum Electron. **QE-2**, 467 (1966).
[40] R. G. Brewer and C. H. Townes, Phys. Rev. Lett. **18**, 196 (1967).
[41] V. V. Korobkin and R. V. Serov, ZhETF Pis. Red. **6**, 642 (1967) [JETP Lett. **6**, 135 (1967)].
[42] V. V. Korobkin, A. M. Prokhorov, R. V. Serov, and M. Ya. Shchelev, ZhETF Pis. Red. **11**, 153 (1970) [JETP Lett. **11**, 94 (1970)].
[43] N. I. Lipatov, A. A. Manenkov, and A. M. Prokhorov, ZhETF Pis. Red. **11**, 444 (1970) [JETP Lett. **11**, 300 (1970)].
[44] M. Maier, G. Wendl, and W. Kaiser, Phys. Rev. Lett. **24**, 352 (1970).
[45] N. Bloembergen, Paper presented at the Esfahan

Symposium on Fundamental and Applied Laser Physics, Iran, August, 1971.
[46] A. L. Dyshko, V. N. Lugovoĭ, and A. M. Prokhorov, Dokl. Akad. Nauk SSSR 188, 792 (1969) [Sov. Phys.-Doklady 14, 976 (1970)].
[47] V. I. Talanov, ZhETF Pis. Red. 11, 303 (1970) [JETP Lett. 11, 199 (1970)].
[48] V. N. Lugovoĭ, Vvedenie v teoriyu vynuzhdennogo kombinatsionnogo rasseyaniya (Introduction to the Theory of Stimulated Raman Scattering), Nauka, M., 1968.
[49] A. D. Kudryavtseva, A. I. Sokolovskaya, and M. M. Sushchinskiĭ, Kvantovaya Elektron. (Moscow) No. 1 (7), 73 (1972) [Sov. J. Quantum Electron. 2, 63 (1972)].
[50] V. S. Butylkin, A. E. Kaplan, and Yu. G. Khronopulo, Izv. Vyssh. Ucheb. Zaved., Radiofiz. 12, 1792 (1969).
[51] M. M. T. Loy and Y. R. Shen, Phys. Rev. Lett. 22, 994 (1969).
[52] M. M. T. Loy and Y. R. Shen, Phys. Rev. Lett. 25, 1333 (1970).
[53] E. Garmire, R. Y. Chiao, and C. H. Townes, Phys. Rev. Lett. 16, 347 (1966).
[54] C. C. Wang, Phys. Rev. Lett. 16, 344 (1966).
[55] V. I. Bespalov and V. I. Talanov, ZhETF Pis. Red. 3, 471 (1966) [JETP Lett. 3, 307 (1966)].
[56] V. E. Zakharov, V. V. Sobolev, and V. S. Synakh, ZhETF Pis. Red. 14, 564 (1971) [JETP Lett. 14, 390 (1971)].
[57] V. E. Zakharov and A. B. Shabat, Tochnaya teoriya dvumernoĭ samofokusirovki i odnomernoĭ avtomodulyatsii voln v nelineĭnykh sredakh (Rigorous Theory of Two-Dimensional Self-Focusing and One-Dimensional Self-Modulation of Waves in Nonlinear Media), Preprint, Institute of Nuclear Physics, Siberian Division, Academy of Sciences of the USSR, Novosibirsk, 1971.
[58] A. V. Gurevich and A. B. Shvartsburg, Zh. Eksp. Teor. Fiz. 58, 2012 (1970) [Sov. Phys.-JETP 31, 1084 (1970)].
[59] A. V. Gurevich, L. V. Pariĭskaya and A. B. Shvartsburg, Zh. Eksp. Teor. Fiz. 61, 1379 (1971) [Sov. Phys.-JETP 34, 733 (1972)].
[60] A. V. Butenin, V. V. Korobkin, A. A. Malyutin, and M. Ya. Shchelev, ZhETF Pis. Red. 6, 687 (1967) [JETP Lett. 6, 173 (1967)].
[61] Y. Kato and H. Takuma, J. Opt. Soc. Amer. 61, 347 (1971).
[62] W. R. L. Clements and B. P. Stoicheff, Appl. Phys. Lett. 12, 246 (1968).
[63] N. M. Kroll, J. Appl. Phys. 36, 34 (1965).
[64] B. Ya. Zel'dovich, ZhETF Pis. Red. 15, 226 (1972) [JETP Lett. 15, 158 (1972)].
[65] V. V. Korobkin, V. N. Lugovoĭ, A. M. Prokhorov, and R. V. Serov, ZhETF Pis. Red. 16, 595 (1972) [JETP Lett. 16, 419 (1972)].
[66] A. A. Abramov, V. N. Lugovoĭ, and A. M. Prokhorov, ZhETF Pis. Red. 9, 675 (1969) [JETP Lett. 9, 419 (1969)].
[67] J. P. Taran and T. K. Gustafson, IEEE J. Quantum Electron. QE-5, 381 (1969).
[68] M. Maier, W. Kaiser, and J. A. Giordmaine, Phys. Rev. Lett. 17, 1275 (1966).
[69] M. Maier, W. Kaiser, and J. A. Giordmaine, Phys. Rev. 177, 580 (1969).
[70] Yu. I. Kyzylasov, V. S. Starunov, and I. L. Fabelinskiĭ, ZhETF Pis. Red. 9, 383 (1969) [JETP Lett. 9, 227 (1969)].
[71] Yu. I. Kyzylasov and V. S. Starunov, ZhETF Pis. Red. 9, 648 (1969) [JETP Lett. 9, 401 (1969)].
[72] E. B. Treacy, Measurement and Interpretation of Dynamic Spectrograms of Picosecond Light Pulses, Preprint, 1972.
[73] F. Shimiza, Phys. Rev. Lett. 19, 1997 (1967).
[74] A. C. Cheung, D. M. Rank, R. Y. Chiao, and C. H. Townes, Phys. Rev. Lett. 20, 786 (1968).
[75] F. DeMartini, C. H. Townes, T. K. Gustafson, and P. P. L. Kelley, Phys. Rev. 164, 312 (1967).
[76] T. K. Gustafson, J. P. Taran, H. A. Haus, J. R. Lifshitz, and P. L. Kelley, Phys. Rev. 177, 306 (1969).
[77] V. N. Lugovoĭ and A. M. Prokhorov, ZhETF Pis. Red. 12, 478 (1970) [JETP Lett. 12, 333 (1970)].
[78] Y. R. Shen and M. M. T. Loy, Phys. Rev. A3, 2099 (1971).
[79] M. M. Denariez-Roberge and J. P. Taran, Appl. Phys. Lett. 14, 205 (1969).
[80] R. Cubeddu, R. Polloni, C. A. Sacchi, O. Svelto, and F. Zaraga, Phys. Rev. Lett. 26, 1009 (1971).
[81] R. Cubeddu and F. Zaraga, Opt. Commun. 3, 310 (1971).
[82] N. G. Bondarenko, I. V. Eremina, and V. I. Talanov, ZhETF Pis. Red. 12, 125 (1970) [JETP Lett. 12, 85 (1970)].
[83] M. A. Bol'shov and G. V. Venkin, Zh. Prikl. Spektrosk. 9, 1050 (1968).
[84] M. M. Bubnov, Diploma Thesis, Moscow State University, 1969.
[85] J. A. Fleck, Jr. and P. L. Kelley, Appl. Phys. Lett. 15, 313 (1969).
[86] A. L. Dyshko, V. N. Lugovoĭ, and A. M. Prokhorov, Zh. Eksp. Teor. Fiz. 65, 1367 (1973) [Sov. Phys.-JETP 38, No. 4 (1974)].
[87] O. Rahn and M. Maier, Phys. Rev. Lett. 29, 558 (1972).
[88] G. K. L. Wong and Y. R. Shen, Appl. Phys. Lett. 21, 163 (1972).
[89] E. Courtens, IEEE J. Quantum Electron QE-8, 588 (1972).
[90] G. A. Askar'yan, Kh. A. Diyanov, and M. M. Mukhamadzhanov, ZhETF Pis. Red. 14, 452 (1971) [JETP Lett. 14, 308 (1971)].
[91] V. V. Korobkin, Usp. Fiz. Nauk 107, 512 (1972) [Sov. Phys.-Uspekhi 15, 520 (1973)].

Translated by A. Tybulewicz